

Long-term marsh growth and retreat in an  
online coupled hydrodynamic,  
morphodynamic and ecological model

**MASTER THESIS IN  
WATER ENGINEERING AND MANAGEMENT  
FACULTY OF ENGINEERING TECHNOLOGY  
UNIVERSITY OF TWENTE**

June 11, 2019

Author: S.J. Odink  
Student number: s1879200  
Location: Enschede

**Graduation Committee**

prof. dr. S.J.M.H. Hulscher	University of Twente
dr. ir. B.W. Borsje	University of Twente
ir. B.P. Smits	Deltares
ir. P.W.J.M. Willemsen	University of Twente

## Abstract

Salt marshes are widely regarded as pristine ecosystems serving multiple ecological functions. Moreover, submerged salt marsh have the ability to attenuate wave energy, which makes them suitable as a natural way of flood protection. Given these positive characteristics coastal engineers, managers and policy makers are looking to preserve and restore these salt marshes in salt marsh creation and restoration projects. However, salt marshes are also known as highly dynamic ecosystems and significant changes in their total covered area have been observed in the past. Even for marshes located in relatively close proximity to each other (a few kilometres apart only) both growth and retreat have been observed over decadal timescales.

Numerical models are often used to simulate the long-term development of salt marsh ecosystems. In most of these models the establishment of new vegetation is either neglected or included as an idealized stochastic function. In such models, each grid cell has an equal chance of vegetation establishment, even though their physical properties i.e. the hydro- and morphodynamic characteristics are different. Recent field and flume experiments suggest that the chances of seedling establishment (i.e. the establishment of new vegetation) may be a function of bed level dynamics. These theories state that if sediment is eroded underneath a seedling with a rate greater than the growth rate of their roots, seedlings will be uprooted and subsequently fail to establish. On the other hand, if sedimentation occurs over a rate which is greater than the growth rate of the seedlings, seedlings will be buried and thus fail to establish as well. The Windows of Opportunity concept accounts for, and describes, this relation between bed level dynamics and seedling establishment. This concept was implemented in a numerical model (D-Flow FM) in order to create a process based vegetation establishment model. The Windows of Opportunity establishment model was combined with a model which governs the growth and decay of established salt marsh vegetation over time. Together, they form a dynamic vegetation model in which the vegetation field is modelled in a process based way.

The model results suggest that the establishment of pioneering vegetation on bare unvegetated mudflats is an important process for the formation of tidal channels. Once a few patches of vegetation are established, flowing water concentrates between these laterally expanding patches of established vegetation. The flowing water increases the bed shear stress leading to erosion which initiates the formation of tidal channels. Due to the erosion between these vegetation patches seedlings are unable to root within these first tidal channel outlines. The rate at which seedlings establish subsequently affects the spatial layout of the tidal channels as well as their width and depth. In case of high vegetation rates, narrow and deep tidal channels are formed which follow the direction of the tidal flow. With slower vegetation rates wider tidal channels are created which are eroded less quickly and show a clear meandering pattern.

The presented model may serve as a reference case for further process based vegetation modelling which could include time-varying physical forcings such as waves or river discharges.



## Contents

1. Introduction.....	7
1.1 State of the art .....	8
1.2 Research gap .....	10
1.3 Research aim .....	11
1.4 Research questions .....	11
1.5 Methods .....	11
1.6 Report outline .....	11
2. Methods.....	13
2.1 Reference location.....	13
2.2 Model Setup.....	14
2.3 Windows of Opportunity framework .....	17
2.4 Population dynamics concept .....	19
2.5 Combining Windows of Opportunity and Population dynamics.....	21
2.6 Timescales .....	22
2.7 Seasonality.....	24
2.8 Seedling availability .....	24
2.9 Run scenarios.....	25
3. Results.....	27
3.1 Default case .....	27
3.2 Different vegetation rates .....	29
3.3 Sea level rise.....	31
4. Discussion .....	34
4. Conclusions.....	37
6. Recommendations.....	39
References .....	41
Appendix A – Hydrodynamic model equations .....	45
Appendix B – Discretization of vegetation diffusion equation.....	46
Appendix C – Vegetation in the hydrodynamic model.....	47
Appendix D – Bed level and vegetation evolution over time for different vegetation rates....	48



## 1. Introduction

Salt marshes are widely recognised as valuable ecosystems, delivering several important ecological functions such as providing habitat to a wide range of flora and fauna (Irmeler et al., 2002; Van Eerden et al., 2005) as well as filtering nutrients and sediments from the waters surrounding these ecosystem (Almeida et al., 2011; Struyf et al., 2006). They are typically found along temperate, low-energy or sheltered shorelines (Allen, 200). Their presence is truly worldwide and conservative estimates on their total covered area go over 5 million hectares (Mcowen et al., 2017). During storm surges, submerged salt marshes have the ability to dissipate wave energy (Möller et al., 2014). Hereby making them suitable as a natural way of flood protection (Borsje et al., 2011). Possibly complementing existing coastal protection solutions such as dikes. Due to the sediment trapping ability of salt marshes salt marshes are able to, within limits, keep up with sea level rise. However, salt marshes are also known as highly dynamic ecosystems and significant changes in their covered area have been observed in the past (Van der Wal et al., 2008; Harmsworth & Long, 1986; Huang et al., 2008). The dynamic behaviour of salt marsh systems is ultimately driven by the physical forces to which these marshes are subjected, in most cases a combination of waves and tides.

Their possible use as a nature-based way of flood protection plus the recognition of the ecological value of these ecosystems has led to multiple salt marsh creation and restoration projects (e.g. Roman & Burdick, 2012; Williams & Faber, 2001). Moreover, protective management regulations for these systems have been put in place. For efficient coastal management and successful implementation of salt marsh systems as a means of coastal protection, a better understanding of the physical processes driving the dynamic behaviour of these systems may be valuable knowledge. This knowledge could for example be used to control and thereby manage the dynamic behaviour of salt marshes.

Quite a substantial amount of research on this topic has already been done. Amongst others with the use of numerical models, analytical models, lab experiments and field studies. The next section will present an overview of the current state of research, which forms the introduction for the research gap and research objective presented at the end of this chapter.

## 1.1 State of the art

Salt marshes are complex natural ecosystems and as such none of them are exactly identical. Geomorphological settings such as coastline shape, tidal range, salinity and sediment characteristic play a role in the landscaping of a marsh (Allen, 2000). Yet common and distinctive patterns can be observed within most marsh landscapes. The vegetation within the marshes is typically dissected by tidal channels. The channels play a key role in the marsh systems since they serve as a pathway for the tidal waters entering the marsh. Given the landward to seaward slope perpendicular to the shoreline, discharge through the channels is usually larger at the seaward side of the marsh and as such channels are generally wider and deeper at the seaward side. Figure 1 presents an aerial image of a full grown salt marsh system located in Vlieland.



Figure 1 Salt marsh in Vlieland (Image: Rijkswaterstaat - Joop van Houdt)

As with most vegetation, the growth of salt marsh vegetation starts with seedlings. The initiation of a salt marsh starts with the colonization of seedlings from pioneer species on a bare mudflat. Within Europe, the dominant salt marsh pioneer species is *Spartina Anglica* or common cordgrass. Despite the harsh conditions in the intertidal area, *Spartina* seedlings have the ability to establish quickly in these conditions (Friess et al., 2012). Once rooted on the mudflat *Spartina* vegetation typically grows in a circular patch (Sánchez et al., 2001). Figure 2 displays these early stages of salt marsh development of a salt marsh system located in the Western Scheldt. Multiple circular patches of *Spartina* tussocks can be observed. Note that these circular patches can also be observed at the edge between the marsh platform and the mudflat in Figure 1. Within the vegetation patches, flow velocities are reduced and suspended sediment is able to settle. The trapped sediment in these patches sets off a positive feedback as the extra sediment favours vegetation growth and further decreases flow velocities. Just outside of these tussocks the water is diverted around the vegetation leading to an increase in flow velocities and the formation of

gullies (van Wesenbeeck, 2007). As these patches grow and laterally diffuse flowing water concentrates between laterally expanding patches of vegetation leading to increased bed shear stresses and possibly erosion. Ultimately this process can lead to the formation of tidal channels (Temmerman et al, 2007).

Once established and fully grown the extra friction in the vegetated parts of the marsh results in a reduction of flow velocities. Especially in the vegetated areas, suspended sediment from the incoming tidal flow is able to settle, leading to a marsh expansion. Generally speaking, this accumulated sediment is only eroded during extreme storm conditions. The expansion of the marsh as a result of the added sedimentation can lead to the formation of a cliff between the vegetated part of the marsh and the bare mudflat since the mudflat is accumulating less sediment. During storm conditions, this often nearly vertical cliff is prone to erosion due to waves breaking onto this cliff. On the other hand, if conditions are calm enough, the unvegetated part in front of the cliff could get colonized, trap suspended sediments as a result of the newly established vegetation and re-emerge again. These processes can result in so called marsh cycles, in which marsh platforms display cycles between growth and erosion (Van der Wal et al., 2008).



*Figure 2 Salt marsh pioneer zone with tussocks of Spartina Anglica (image: van Wesenbeeck, B.K., 2007)*

The aforementioned processes such as establishment, expansion and erosion of vegetation are known to develop and steer the marsh platform evolution over decadal timescales. The decadal evolution of these systems makes the study of these processes difficult. Field data from measurements carried out over such long periods is scarce. It is at this point that numerical modelling comes in. Using numerical models it is possible to simulate the long term development of salt marsh ecosystems in order to better understand them. Quite a few studies have already been executed using numerical models. For example the channel initiation and evolution process as a result of flow-vegetation feedback which is modelled in multiple studies (e.g. D'Alpaos et al., 2007; Schwarz et al., 2018; Temmerman et al., 2007). In these publications a physical explanation for the spatiotemporal differences in erosion and

sedimentation rates within the marsh is theorised and modelled. The model results agree fairly well with field data on erosion and sedimentation rates. Some models tried modelling the lateral dynamics of salt marshes. For example the study of Mariotti and Fagherazzi (2010) in which an empirical relationship relating wave energy to marsh cliff erosion in a numerical model was used to study the long-term evolution of the marsh cliff. This leads to conditions (combination between sea level rise and sediment availability) under which the marsh cliff may expand or retreat. More recently Best et al. (2018) developed a numerical model to assess the resilience of salt marsh ecosystems under different rates of sea level rise. Each of these models have their own strengths and weaknesses. The way of inclusion of vegetation usually is a common weakness in these models. In most models, the salt marsh vegetation is included as a static vegetation field. In this case the vegetation field, and thus the effect of vegetation on flow and morphology, is constant over time. Some models such as Schwarz et al. (2018) and Temmerman et al. (2007) do contain a dynamic vegetation field in which the vegetation field is altered depending on the hydro- or morphodynamic conditions. However, in these models the establishment of new vegetation is included as a stochastic chance function. Meaning that each grid cell has an equal chance of vegetation establishment, even though their physical properties i.e. the hydro- and morphodynamic characteristics are different.

The physical processes responsible for marsh expansion as a result of colonisation by pioneering species were recently theorised by Hu et al. (2015) and Bouma et al. (2016). Hu et al. (2015) used the recently developed Windows of Opportunity (WoO) theory which assumes that the magnitude of bed shear stress over time at a certain location determines the successfulness of seedling establishment at that location. The theory was implemented in an analytical hydrodynamic model. The model was able to, in some degree, recreate observed spatial variability in lateral marsh expansion (i.e. establishment of new vegetation). The theory of Bouma et al. (2016) states that short term sediment dynamics negatively affect the chances of successful seedling establishment. They tested and confirmed their theory in a field experiment. Recently, Poppema et al. (2019) altered the original WoO theory of Hu et al. (2015) to a framework in which inundation time and bed level dynamics determine whether *Spartina* seedlings can establish. The framework was implemented in a numerical model to study which locations within the intertidal area are suitable for vegetation establishment. Importantly, the numerical model was not used to study the morphological evolution of a salt marsh as a result of the actual establishment.

## 1.2 Research gap

Numerical models can serve as a valuable tool for studying the decadal evolution of salt marshes. Multiple numerical salt marsh models can be found in literature. In most of these models, the establishment of new vegetation is either not included at all or included as a rather idealised stochastic function. Recent publications of amongst others Hu et al. (2015) and Bouma et al. (2016) presented vegetation dynamics theories that may give a better understanding on the physical processes facilitating establishment of new vegetation. However, these vegetation dynamics theories have only been partly included in existing numerical models on salt marsh dynamics. Poppema et al. (2019) demonstrated that it is possible to implement a dynamic vegetation theory in a numerical model. The inclusion of such theory in existing numerical models can potentially lead to more process based or less idealised models. Such a process based model may aid in studying the physical forcings driving the decadal dynamic behaviour of salt marshes. And they could thus serve as a valuable tool for coastal engineers, managers and policy makers who are aiming to preserve these ecosystems, or looking to create new ones.

### 1.3 Research aim

The goal of this thesis is to fill in the research gap that was identified. To this end, the following research aim is established:

*“To study the physical processes driving the decadal dynamic behaviour of salt marshes by implementing a dynamic vegetation theory in a numerical model”*

### 1.4 Research questions

In line with the formulated research aim the following research questions are established.

1. How can the influence of hydro- and morphodynamics on salt marsh vegetation dynamics, and specifically on the establishment of new vegetation, be included in a numerical model?
2. How can we get confidence in the model results?
3. How can sea level rise be incorporated in a dynamic vegetation model, and how does this affect the salt marsh evolution?

### 1.5 Methods

The research questions will be answered with the use of the following methods. First of all a reference location for the input of the numerical model and vegetation model is selected. With the use of the reference location and previous numerical models a representative input for the hydro- and morphodynamic model is determined. A dynamic vegetation model is constructed by combining the work of Temmerman et al. (2007) and Poppema et al. (2019) forming a newly created ecological model. With the hydrodynamic, morphodynamic and ecological model set out multiple scenarios are composed and run. The results from these scenarios form the basis for the results, discussion and recommendations.

### 1.6 Report outline

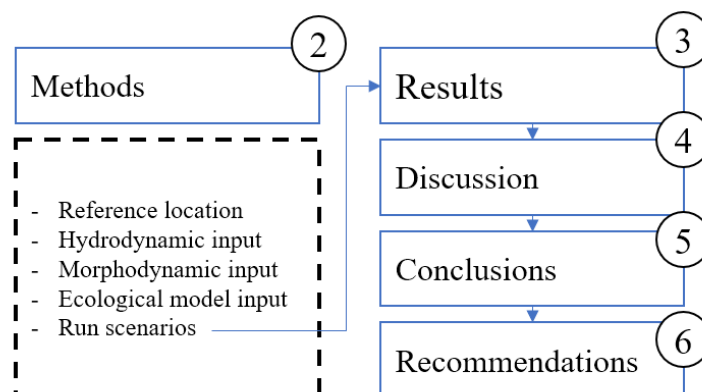


Figure 3 Report outline



## 2. Methods

### 2.1 Reference location

The Western Scheldt estuary was chosen as a reference area for the model parameters. This area was chosen since multiple salt marsh ecosystems located in the Western Scheldt have displayed dynamic behaviour in the past (Van der Wal et al., 2008). A wide variety of field data of the Western Scheldt is available (e.g. typical flow velocities, sediment characteristics, bathymetric data, wave characteristics, vegetation characteristics) (e.g. Callaghan et al., 2010; Vuik et al., 2018; Willemsen et al., 2018). And lastly, in several previous salt marsh modelling studies the Western Scheldt area was used as reference location as well (Attema, 2014; Best et al., 2018; Schwarz et al., 2018; Temmerman et al., 2005). The model descriptions and input parameters given in these publications can be used as a reference for this model. The Western Scheldt contains multiple salt marsh ecosystems. From lower part of the estuary up to Dutch-Belgian border several marshes can be identified, see Figure 4.

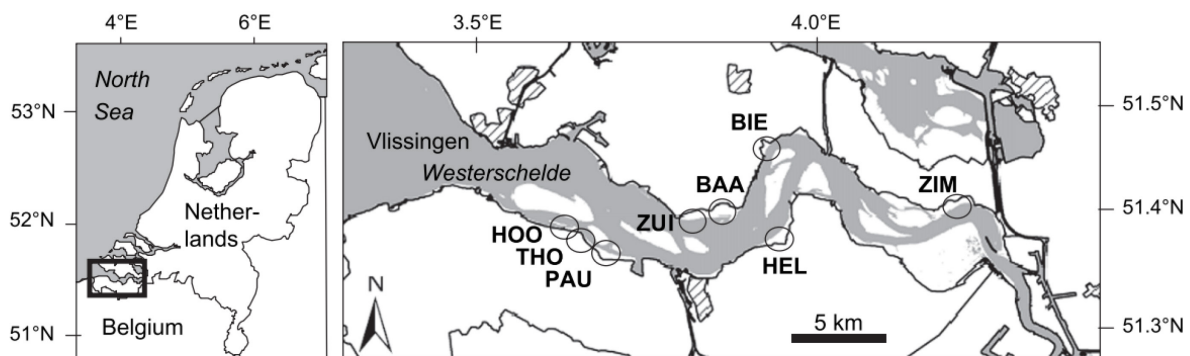


Figure 4 Locations of several salt marshes in the Western Scheldt estuary. Hoofdplaat (HOO) Thomaesolder (THO), Paulinapolder (PAU), Zuidgors (ZUI) Baarland (BAA), Biezelingsche Ham (BIE), Hellegatpolder (HEL), Zimmermanpolder (ZIM). Image: Van der Wal et al. (2008)

The difference in location between the marshes in the Western Scheldt results in differences in physical properties between these marshes. The estuary is subjected to a semi-diurnal tide, the mean tidal range varies between 3.8 metres at Vlissingen to 5.0 metres at Antwerp (Baeyens et al., 1997). The estuary contains fine sediments with sizes ranging between 24  $\mu\text{m}$  to 56  $\mu\text{m}$  in the channels and mudflats and cohesive sediment fractions with particle sizes around 88  $\mu\text{m}$  in the vegetated areas (Best et al., 2018). Common pioneering species in the Western Scheldt are perennial common cord grass (*Spartina Anglica*) and annual glasswort (*Salicornia spp.*). Higher up in the marshes common saltmarsh grass (*Puccinellia maritima*), annual seablite (*Suaeda maritima*) and sea aster (*Aster tripolium*) vegetation can be found (Willemsen et al., 2018). In the period between 1973 and 1986 the average annual mud supply was around 380 kT yr<sup>-1</sup>. After the construction of wastewater treatment plants, weirs, sluices and other man-made structures the mud supply decreased significantly. Between 1992 and 1997 the mud supply varied between 75 and 250 kT yr<sup>-1</sup> (Van Kessel et al., 2011). Wave heights vary depending on the location in the cross-shore direction, with lower wave heights within the marsh and higher wave heights around the tidal flats. Moreover, a clear seasonal pattern in wave heights is observed. In a field study containing four salt marshes located in the Western Scheldt an average wave height of 8 cm during the summer and an average of 17 cm during the winter was observed around the tidal flats. The 5% highest waves consisted of waves with peak wave heights of over 37 cm (Callaghan et al., 2010).

## 2.2 Model Setup

The D-Flow Flexible Mesh (D-Flow FM) model is used to solve the two-dimensional depth-averaged shallow water equations for momentum and continuity for unsteady and incompressible turbulent flow (Deltares, 2019). The full hydrodynamic model equations are presented in appendix A. The depth averaged approach is used in multiple previous salt marsh models (Attema, 2014; Best et al., 2018; Schwarz 2018; Temmerman et al., 2005). A depth-averaged model significantly reduces computational time compared to a three dimensional model (Horstman et al., 2015). As well, the three dimensional mode was simply not yet developed for D-Flow FM at the time of writing. The Partheniades-Krone (Partheniades, 1965) formulation is used for sediment calculations (erosion and sedimentation) of fine, cohesive sediments. The model domain consists of a structured rectangular grid of 144 by 200 cells. Each grid cell is 7x7 metres in size, so the domain captures an area of 1008 metres in width and 1400 metres length. The domain size is chosen such that it represents a marsh in the Western Scheldt. BAA, HEL and PAU, see Figure 4, all have a width of around a kilometre. Wider marshes can be found as well, e.g. ZIM and ZUI both have a width of around two kilometres. Yet, these marshes do not visibly display different characteristics (channel width and length, vegetation pattern) compared to the smaller marshes. The domain width and cell sizes should enable the formation of channel patterns. In the model of Best et al. (2018) a domain width of 500 metres and grid cell size of 10x10 metres was sufficient for the formation of channels patterns, smaller grid sizes did not qualitatively alter their results. Although the Flexible Mesh suite enables the creation of flexible meshes (e.g. triangular grid cells), a structured grid is chosen since a structured grid is perfectly smooth and orthogonal which aids in computational time. Several runs with unstructured grids were carried out as well. These runs did not qualitatively look different compared the runs carried out using a structured grid. The domain length of 1400 metres is large enough to include a cross-shore profile with a vegetated platform, tidal flat and a gradually sloping bathymetry up to the deepest point in the adjacent channel. The bathymetry is based on a transect of the Zuidgors (ZUI in Figure 4) salt marsh. The crossshore delta (i.e. distance between two samples point) of these transects is five metres. A single transect located central in the salt marsh was used as a reference for a slightly more idealised transect. As such a smooth uniform bathymetry is created over the alongshore direction. Figure 5 displays a cross-shore transect of the used bathymetry.

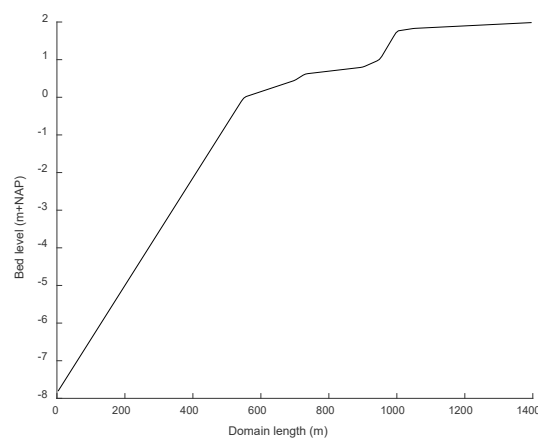


Figure 5 Transect of the initial bathymetry

### *Morphodynamic input*

Similar to Poppema et al. (2019) a uniform manning roughness coefficient of  $0.023 \text{ s m}^{-1/3}$  is used. The manning roughness coefficient is chosen as it accounts for the water depth for determining the roughness, which results in less erosion in the intertidal area as opposed to a uniform roughness coefficient (i.e. a uniform Chézy roughness) of similar magnitude. For the horizontal eddy viscosity and diffusivity a value of  $10 \text{ m}^2 \text{ s}^{-1}$  is used which is typical for these grid sizes and similar to what Willemsen et al. (2016) and Poppema et al. (2019) used for mangrove/mudflat models with similar grid sizes. An initial sediment thickness of 1.5 metres is used for the area in the model domain suitable for vegetation growth. This is the area located between  $1\text{m}+\text{NAP}$  and  $2\text{m}+\text{NAP}$ . For the rest of the domain a sediment thickness of 0.1 metres is chosen. These thicknesses allow for the creation of tidal channels in the area suitable for vegetation growth whilst preventing excess erosion (unrealistically deep tidal channels or channels which carry over through to the rest of the domain). The model contains a single cohesive sediment fraction. As described previously these fine sediments are typical for the Western Scheldt estuary and especially for the area of interest, being the vegetated parts in the intertidal area. Table 1 contains the parameter values used for this single sediment fraction.

<b>Parameter</b>	<b>Description</b>	<b>Value [unit]</b>	<b>Reference</b>
$\rho_{\text{sed}}$	Specific density sediment	2650 [ $\text{kg m}^{-3}$ ]	Best et al. (2018)
$P_{\text{bed}}$	Dry bed density	500 [ $\text{kg m}^{-3}$ ]	Best et al. (2018)
$\tau_{\text{cr,e}}$	Critical bed shear stress for erosion	0.5 [ $\text{N m}^{-2}$ ]	Best et al. (2018)
$\tau_{\text{cr,s}}$	Critical bed shear stress for sedimentation	1000 [ $\text{N m}^{-2}$ ]	Best et al. (2018)
$W_s$	Settling velocity	$5 \cdot 10^{-4}$ [ $\text{m s}^{-1}$ ]	Best et al. (2018)
$M$	Erosion parameter	$5 \cdot 10^{-5}$ [ $\text{kg m}^{-2} \text{ s}^{-1}$ ]	Best et al. (2018)

*Table 1 Sediment input parameters*

The bed level is updated instantly, i.e. every timestep. For every timestep the computed erosion and sedimentation rates are multiplied with a factor of 100 (morphological factor) in order to simulate the desired decadal timescale whilst limiting computational time. A morphological factor of 100 is similar to what is used by many previous authors who used numerical modelling to study the long term (decadal) evolution of salt marshes. Attema (2014), Best et al. (2018) and Schwarz et al. (2018) used a morphological factor of 100, 100 and 91.25 respectively.

### *Hydrodynamic input*

Although waves are important for the area of interest the model is solely forced by tides. Leaving out waves was necessary due to model availability and model runtime. For a reflection on the consequences of this decision please see the discussion. Tides are forced at the only open boundary along the model domain which is located at the channel side of the domain (along the domain width for domain length = 0 metres, see Figure 5). Even though the Western Scheldt estuary is subjected to a spring neap tidal cycle, the model is forced by a single M2 tide with an amplitude of 2.3 metres and a period of 12 hours. A single tidal boundary was opted for since this simplifies the coupling with the vegetation model, as will be discussed in the following section. The influence of vegetation on the hydrodynamics is accounted for by means of a roughness predictor in which vegetation presence is parameterized using a representative bed roughness. The equations can be found in Appendix C. In these equations, a higher value of vegetation biomass, that is density times height times diameter, results in a larger representative

bed roughness (lower chézy coefficient). Furthermore, the equations account for differences in roughness for submerged and unsubmerged vegetation. Unsubmerged vegetated grid cells will display a higher bed roughness as opposed to submerged grid cells with the same amount of vegetation of biomass.

### 2.3 Windows of Opportunity framework

As with all vegetation, establishment of new salt marsh vegetation on bare unvegetated grounds starts with dispersion of seedlings. However, availability of seedlings alone does not guarantee successful establishment. The period between seedling dispersal and mature vegetation should consist of a period in which conditions such as temperature, humidity, winds and waves remain within some sort of threshold which the seedlings can handle.

The Windows of Opportunity (WoO) framework as described by Poppema et al. (2019) can be used as a model that describes and accounts for some of the conditions governing establishment of vegetation. The framework is an extension of the WoO concept originally developed by Balke et al. (2011), which stated that mangrove seedlings can establish given that the hydrodynamic conditions remain below a certain threshold. In the original concept, this threshold is based on the amount of bed shear stress. The theory states that over time seedlings become more rooted and are subsequently able to withstand higher levels of bed shear stress. However, according to Hu et al. (2015) failure of *Spartina anglica* seedlings mainly occurs as a result of erosion of sediment. This sensitivity of *Spartina* seedlings to erosion was also demonstrated in flume experiments. Bouma et al. (2016) and Cao et al. (2018) placed *Spartina* seedlings in a delta flume and subjected them to currents. The experiments showed that the seedlings are very sensitive to erosion. Bed shear stress does relate to erosion since high levels of bed shear stress generally results in higher levels of erosion. Yet, as Poppema et al. (2019) pointed out, slow but continuous erosion can result in high levels of erosion without high peaks of bed shear stress occurring. As such, Poppema et al. (2019) altered the WoO framework to better include the effect of (short-term) sediment dynamics on the successfulness of seedling establishment in the WoO framework.

The extended Windows of Opportunity framework of Poppema et al. (2019) consists of three windows. The first window is a short inundation free-period for roots to grow. In the second windows, plants require calm conditions in order not to be uprooted. This second window consists of limits for the short and long-term bed level dynamics. In the third and final window, mature plants need to withstand mature erosion and sedimentation limits. Figure 6 gives an impression of these requirements. The abbreviations and their meanings will be explained on the next page.

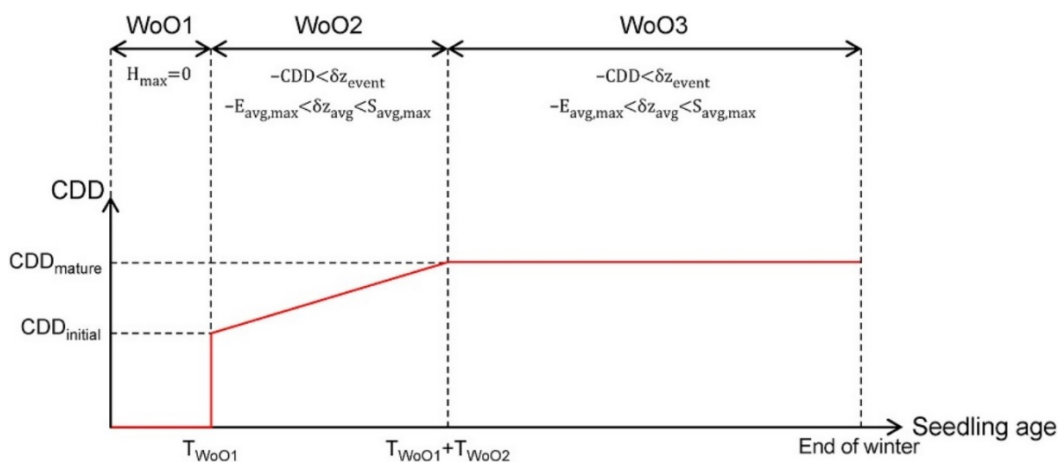


Figure 6 Visualisation of the Windows of Opportunity framework by Poppema et al. (2019) showing the different windows (WoO1, WoO2 and WoO3) over time and the conditions which should be met for successful establishment

Window 2 and 3 thresholds

$$-CDD < \delta z_{event} \quad (1)$$

$$-E_{avg,max} < \delta z_{avg} < S_{avg,max} \quad (2)$$

The thresholds on bed level dynamics in the second window consists of limits on short term bed level dynamics ( $\delta z_{event}$ ) and average bed level dynamics ( $\delta z_{avg}$ ). The short term bed level change should be below the critical disturbance depth (CDD). The CDD is defined as the net bed level erosion (difference between sedimentation and erosion) occurring over a short timeframe. More precisely a timeframe in which no significant plant growth occurs (i.e. days to a week). Erosion greater than the CDD can cause the seedling to topple over (Bouma et al. 2016). The CDD increases over time as seedlings grow and become more rooted. Equation three is used to determine the CDD for each grid cell for each point in time. In this equation  $CDD_{initial}$  depicts the critical disturbance depth at the start of window 2.  $CDD_{mature}$  describes the critical disturbance depth for mature vegetation. The values of these parameters are based on lab experiments on *Spartina Anglica* species executed by Poppema et al. (2019). Apart from these empirical parameters, the value of the CDD depends on the bed level change during the seedlings life ( $\delta z_{life}$ ). Since, if sedimentation occurred over this lifespan, more sediment can be eroded before the seedlings are uprooted. Furthermore, seedlings can compensate for erosion by growing longer roots (Cao et al. 2018).

$$CDD = CDD_{initial} + \frac{t - T_{WoO1}}{T_{WoO2}} * (CDD_{mature} - CDD_{initial}) + \alpha * \delta z_{life} \quad (3)$$

The long term erosion and sedimentation limits described in equation two check whether the sedimentation or erosion exceeds growth rate of plants. If per unit of time, a bed level change (positive or negative) occurs that is greater than the growth rate of plants the plants will either be buried and fail, or roots will be uncovered and subsequently the plants will fail as well. Table 2 displays the values of the WoO parameters as used by Poppema et al. (2019).

Parameter	Description	Value [unit]	Reference
t	Time	[days]	-
$T_{WoO1}$	Duration of window 1	2.5 [days]	Hu et al. (2015)
$T_{WoO2}$	Duration of window 2	80 [days]	Bouma et al. (2016)
$E_{avg,max}$	Long-term erosion limit	5 [mm week <sup>-1</sup> ]	Cao et al. (2018)
$S_{avg,max}$	Long-term sedimentation limit	15 [mm week <sup>-1</sup> ]	Cao et al. (2018)
$CDD_{initial}$	CDD at the start of Window 1	16 [mm]	Poppema et al. (2019)
$CDD_{mature}$	CDD of mature vegetation	23 [mm]	Poppema et al. (2019)
$\alpha$	Sensitivity to bed level change	1.05 [-]	Poppema et al. (2019)
$\delta z_{life}$	Total bed level change over the seedlings life	[mm]	-

Table 2 WoO Parameter values

## 2.4 Population dynamics concept

Growth and decay of vegetation can be included by means of the population dynamics concept. The population dynamics concept was first described by Temmerman et al. (2007) and later used and altered by amongst others Attema (2014) and Schwarz et al. (2018). The population dynamics concept as described in Temmerman et al. (2007) consists of five differential equations (see equation 4) which together account for the temporal change in stem density in a given grid cell. Each equation accounts for a physical process. As such, the concept includes (5) initial plant establishment in bare grid cells, (6) lateral expansion of plants to neighbouring cells, (7) logistic growth of stem densities, (8) plant mortality due to flow stress and (9) plant mortality due to inundation stress.

$$\frac{\partial n_b}{\partial t} = \left(\frac{\partial n_b}{\partial t}\right)_{est} + \left(\frac{\partial n_b}{\partial t}\right)_{diff} + \left(\frac{\partial n_b}{\partial t}\right)_{growth} - \left(\frac{\partial n_b}{\partial t}\right)_{flow} - \left(\frac{\partial n_b}{\partial t}\right)_{inund} \quad (4)$$

$$\left(\frac{\partial n_b}{\partial t}\right)_{est} = P_{est} n_{b,est} \quad (5)$$

$$\left(\frac{\partial n_b}{\partial t}\right)_{diff} = D \left( \frac{\partial^2 n_b}{\partial x^2} + \frac{\partial^2 n_b}{\partial y^2} \right) \quad (6)$$

$$\left(\frac{\partial n_b}{\partial t}\right)_{growth} = r \left( 1 - \frac{n_b}{K} \right) n_b \quad (7)$$

$$\left(\frac{\partial n_b}{\partial t}\right)_{flow} = \begin{cases} PE_{\tau}(\tau - \tau_{cr,p}) & \text{when } \tau > \tau_{cr,p} \\ 0 & \text{when } \tau \leq \tau_{cr,p} \end{cases} \quad (8)$$

$$\left(\frac{\partial n_b}{\partial t}\right)_{inund} = \begin{cases} PE_H(H - H_{cr,p}) & \text{when } H > H_{cr,p} \\ 0 & \text{when } H \leq H_{cr,p} \end{cases} \quad (9)$$

In equation 5,  $\frac{\partial n_b}{\partial t}$  represents the time derivative of the stem density in a given grid cell. Establishment of new vegetation occurs randomly with a certain chance of establishment  $P_{est}$ . If establishment occurs the newly established tussock will have a stem density of  $n_{b,est}$ . Once established, stem densities diffuse laterally over both x and y direction with a plant diffusion coefficient D. Stem densities grow with a logistic growth rate r up to the maximum carry capacity K. Lastly, stem densities decay with a mortality coefficient related to flow stress  $PE_{\tau}$  and inundation stress  $PE_H$  given that the bed shear stress  $\tau$  or inundation depth  $H$  in a certain grid cell is higher than the critical bed shear stress  $\tau_{cr,p}$  or critical inundation height  $H_{cr,p}$ .

The differential equation in equation 6 should be discretized in order to be implemented in the numerical model. The discretized equation used in the model is presented in Appendix A.

Temmerman et al. (2007) used the values displayed in Table 3 for the application of the population dynamics concept. These values were used to model *Spartina Anglica* vegetation.

<b>Parameter</b>	<b>Description</b>	<b>Value [unit]</b>	<b>Reference</b>
$n_b$	Vegetation stem density	[stems m <sup>-2</sup> ]	-
t	Time	[s]	-
$P_{est}$	Chance of establishment	0.01 [yr <sup>-1</sup> ]	Van Hulzen et al. (2007)
$n_{b,est}$	Stem density of newly vegetated grid cells	200 [stems m <sup>-2</sup> ]	Van Hulzen et al. (2007)
D	Diffusion coefficient	0.2 [m <sup>2</sup> yr <sup>-1</sup> ]	Van Hulzen et al. (2007)
r	Intrinsic growth rate of stem density	1.0 [yr <sup>-1</sup> ]	Van Hulzen et al. (2007)
K	Carrying capacity of stem density	1200 [m <sup>-2</sup> ]	Temmerman et al. (2005)
$\tau_{cr,p}$	Critical bed shear stress	0.26 [N m <sup>-2</sup> ]	Van Hulzen et al. (2007)
$H_{cr,p}$	Critical inundation depth	1.1 [m]	Van Huzlen et al. (2007)

Table 3 Population dynamics parameters

## 2.5 Combining Windows of Opportunity and Population dynamics

Both the windows of opportunity and population dynamics concept provide a framework for dynamic vegetation modelling. Each of these frameworks have their own strengths and weaknesses. The population dynamics concept is extensive in the sense that it includes both vegetation growth as well as decay. Furthermore it includes lateral diffusion of vegetation, a process also observed in practice, see for example Sánchez et al. (2001). A weakness of the population dynamics concept would be the random establishment of new vegetation, which occurs purely depending on a chance function and regardless of the hydro- and morphodynamic conditions. Meaning that the chance of establishment in a grid cell located on the mudflat that is subjected to large bed shear stresses and long inundation periods would be equal to the chance of establishment in a grid cell located higher up in the marsh subjected to significantly lower bed shear stresses and inundation periods. On the other hand, the Windows of Opportunity framework as described by Poppema et al. (2019) accounts for the notion that establishment of vegetation may be a function of the magnitude of hydro and morphodynamic activity. However, this version of the WoO framework does not include vegetation growth. As well, decay of vegetation occurs solely as a function of bed level dynamics. Furthermore, as the thresholds on bed level dynamics in the third window are surpassed, vegetation is assumed as failed. In other words, vegetation decay in this WoO framework is not included as a gradual process but rather as an instant process.

One could hypothesize that by combining the Windows of Opportunity and Population dynamics frameworks a more realistic or process based dynamic vegetation model is created. The process based WoO framework can be used to replace the stochastic chance function governing the establishment of new vegetation in the Population dynamics framework. In the population dynamics model, the random establishment of vegetation (equation 5) would vanish since establishment of new vegetation would occur according to the WoO framework. As well, one should determine from whereon the population dynamics model ‘takes over’ from the WoO model. From that point onward, the population dynamics model would regulate both the growth and decay of vegetation. It is opted to mark the end of Window 2 as the switching point between both models. At this point vegetation is assumed as established in the WoO framework. Subsequently growth and decay of established vegetation would occur according to the population dynamics model. Figure 7 gives an impression on how the combination of both models would function over time.

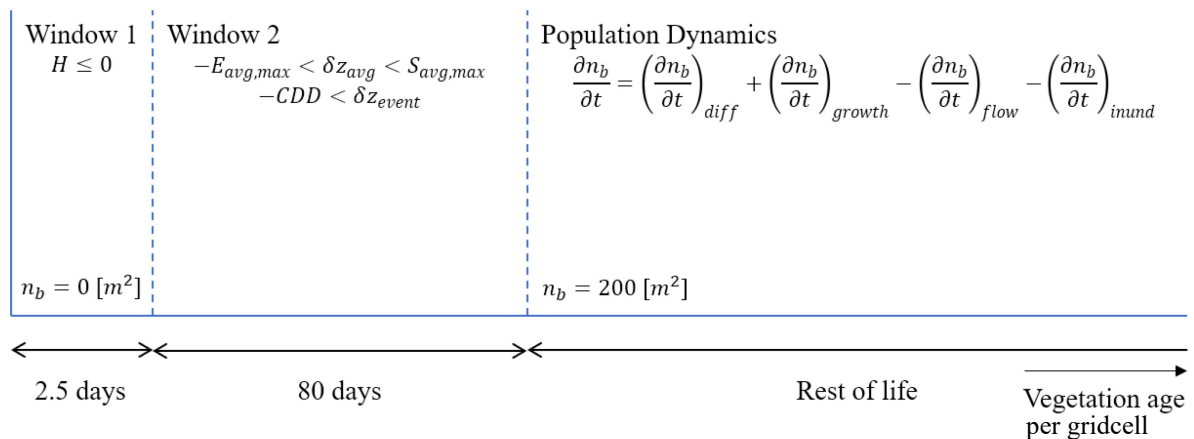


Figure 7 Combined WoO (Poppema et al., 2019) and Population Dynamics (Temmerman et al., 2007) vegetation model displaying the conditions in window 1 plus window 2 which should be fulfilled in order for vegetation to establish and the population dynamics equations governing the temporal variation in stem densities

Figure 7 displays how the combined dynamic vegetation model enables establishment combined with growth and decay of vegetation. It should be noted that if the conditions in a grid cell exceed the thresholds of Window 1 or Window 2, the vegetation age resets and start at  $t = 0$  days again. As well, once established vegetation (vegetation age  $> 82.5$  days) has vanished ( $n_b \leq 0$ ) at any point in time as a result of the inundation stress and flow stress terms of the population dynamics model the vegetation age resets and subsequently starts at  $t = 0$  days as well. The vegetation characteristics (age and density) are determined per gridcell.

## 2.6 Timescales

To implement the aforementioned combined vegetation model in the hydro- and morphodynamic model a challenge arises regarding the timescales of the different processes. The hydrodynamic, morphodynamic and ecological evolution are known to influence each other. However, in the model these processes occur over different timescales. The first timescale that can be identified is the hydrodynamic timescale. For example, in the case of semi-diurnal tides (and an assumed spring-neap period of 15 days) over the course of 300 days 20 spring neap cycles occur. Yet, as result of the used morphological factor of 100 the morphological evolution over a period of 30.000 days is modelled. Figure 8 gives an impression on the relation between the hydro- and morphodynamic timescale.

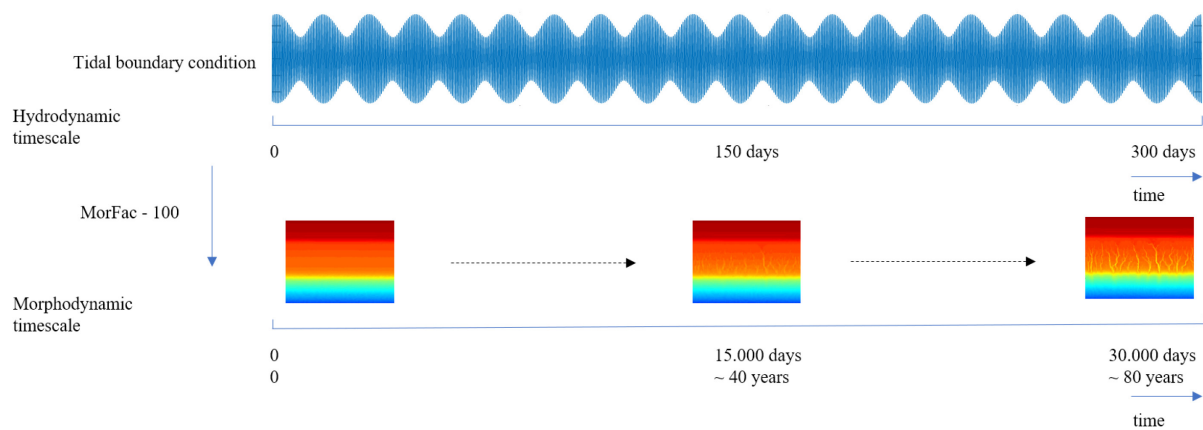


Figure 8 Illustration of the relation between a hydro- and morphodynamic timescale

The combined vegetation model requires 2.5 days free of inundation followed up by a period of 80 days in which bed level dynamics stay within the thresholds of window 2 (equation 1, 2 and 3) for new vegetation to establish. The question that subsequently arises is how these requirements transform to the hydro- and morphodynamic timescale. It seems that there is no logical solution to this problem. The most ‘realistic’ solution would be to not use a morphological factor at all. In such scenario all processes would occur over the same timescale and no transformation of timescales is needed. Unfortunately this option would increase the computational time needed with a factor 100 to undesirable lengths. As already discussed in section 2.2, a single tidal boundary was opted for as this simplifies the coupling of the timescales. The single tidal boundary ensures daily morphological activity, as the marsh platform is inundated during every tidal cycle. The actual spring-neap tidal boundary should however be accounted for considering the requirements of window 1. These requirements state that a seedling requires 2.5 days free from inundation. With a single tidal boundary, the only grid cells that would surpass such requirements would be grid cells located above the maximum water level of the tidal boundary. As such, it was opted to construct an artificial spring-neap tidal boundary. This boundary is not used in the hydro- or morphodynamic model but only used

to check the requirements of Window 1, see Figure 9. This ensures that grid cells located higher up in the marsh have greater chances of passing the requirements of W1 as opposed to grid cells located at lower elevations which (in practice!) are inundated more frequently.

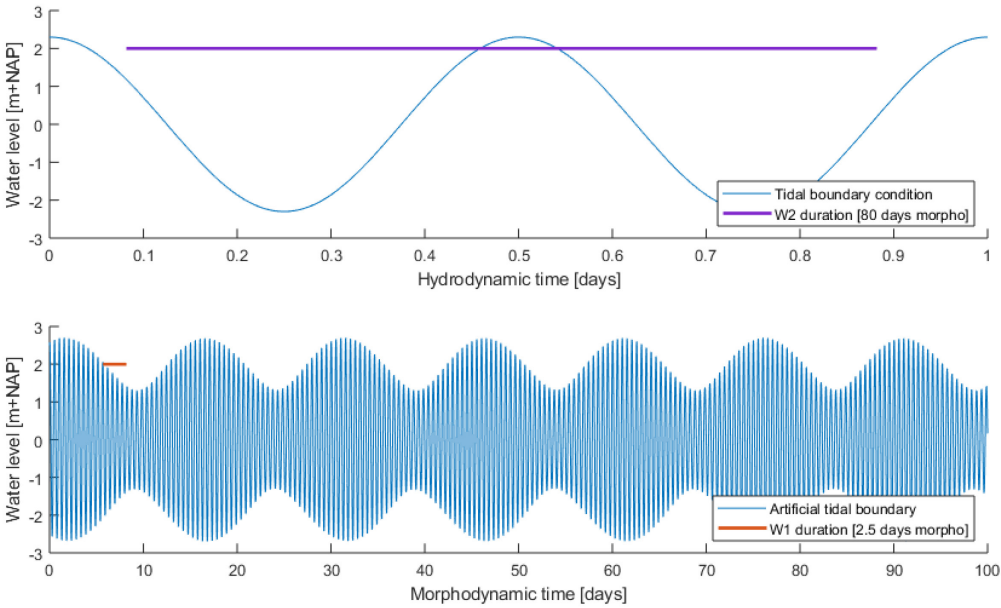


Figure 9 Illustration of W1 following an artificial tidal boundary constructed over the morphodynamic timescale and W2 following the morphodynamic timescale for a grid cell located at  $z=2\text{ m} + \text{NAP}$ .  $\text{MorFac} = 100$



To account for seedling availability in the dynamic vegetation model a simple chance function determines if a grid cell actually ends up vegetated after passing the requirements of the WoO model. The parameter is expressed in percentages per year. For the default case this parameter is set to 2%. This means that, per year, seedlings will colonize 2% of the grid cells that pass the requirements of the WoO model. Such colonization rate is of similar magnitude as the stochastic parameters of Schwarz et al. (2018) and Temmerman et al. (2007).

## 2.9 Run scenarios

Three different scenarios with different setups were run. The first scenario serves as a default or reference case. In the second scenario, the seedling availability parameter is altered to study the effect of different vegetation rates on the salt marsh evolution, similar to the study of Schwarz et al. (2018), see section 2.8. In the last scenario the developed profile and vegetation pattern from the default case after 50 years is used as the starting conditions for modelling another 100 years over which the average sea level rises with 0.01 metres per year. Such sea level rise rate is at the lower spectrum of projected sea level rise rates. However, as the model setup does not contain an inflow of suspended sediments the vertical marsh expansion is limited and a sea level rise of 1 metre is high enough to completely drown the salt marsh.

Scenario	Seedling availability (see section 2.8)	Initial profile	Sea level rise
1	2%	Initial transect (see Figure 5)	None
2	1%, 4%, 8%	Initial transect (see Figure 5)	None
3	2%	Developed profile from scenario #1 after 50 years	0.01 m yr <sup>-1</sup>

*Table 4 Run scenarios*



## 3. Results

### 3.1 Default case

The model was run with the default setup and parameters as described in the method (scenario 1). Figure 11 displays the evolution of the part of the domain that is suitable for vegetation growth, roughly the area between 1m+NAP and 2m+NAP. As visible in Figure 11, the establishment of vegetation results in a convergence of flow between established patches of vegetation resulting in an increase in bed shear stress between the vegetation. As these patches of vegetation grow and diffuse this convergence increases which further increases the bed shear stresses and leads to the formation of channels. At around 50 years nearly the entire platform is covered with vegetation, except for the locations in which a tidal channel is present. The sediment that is eroded from the tidal channels is redistributed over the domain. The largest part of this sediment ends up on the mudflat which results in a lateral expansion of the salt marsh in the seaward direction. A portion of this eroded sediment is deposited in the back of the marsh (i.e. close to the land boundary) resulting in a vertical marsh expansion. After 50 years, the ecological development halts as there is no more space for further expansion. The unvegetated grid cells are inundated too frequently for vegetation to pioneer or diffuse. Nearly all tussocks have reached their carrying capacity of 1200 stems  $m^{-2}$ . Further morphological evolution is hampered as the maximum bed shear stresses are significantly lower than the critical bed shear stress for erosion, or no more sediment is available for erosion. On the mudflat, bed shear stresses sufficiently high for erosion to occur are visible due to a large outflow of water from the densely vegetated platform. However, since the initial sediment thickness of the mudflat is limited (0.1 metre) this only partly results in the formation (or continuation) of tidal channels on the mudflat. The large amount of sedimentation on the mudflat highlights a weakness of the current model setup. As the model is only forced by tides, only the concentration of flow between patches of vegetation (and thus only the flow through the vegetated platform) is high enough to keep sediment in suspension. As soon as the water reaches the mudflat, flow velocities drop significantly and sediment starts to settle. This is visible by the clear red patches in the bed level plot of Figure 11. As the flowing water finds the path of the least resistance these ‘humps’ of mud on the mudflat form an extra obstacle and result in a meandering channel pattern at the edge between vegetated platform and mudflat.

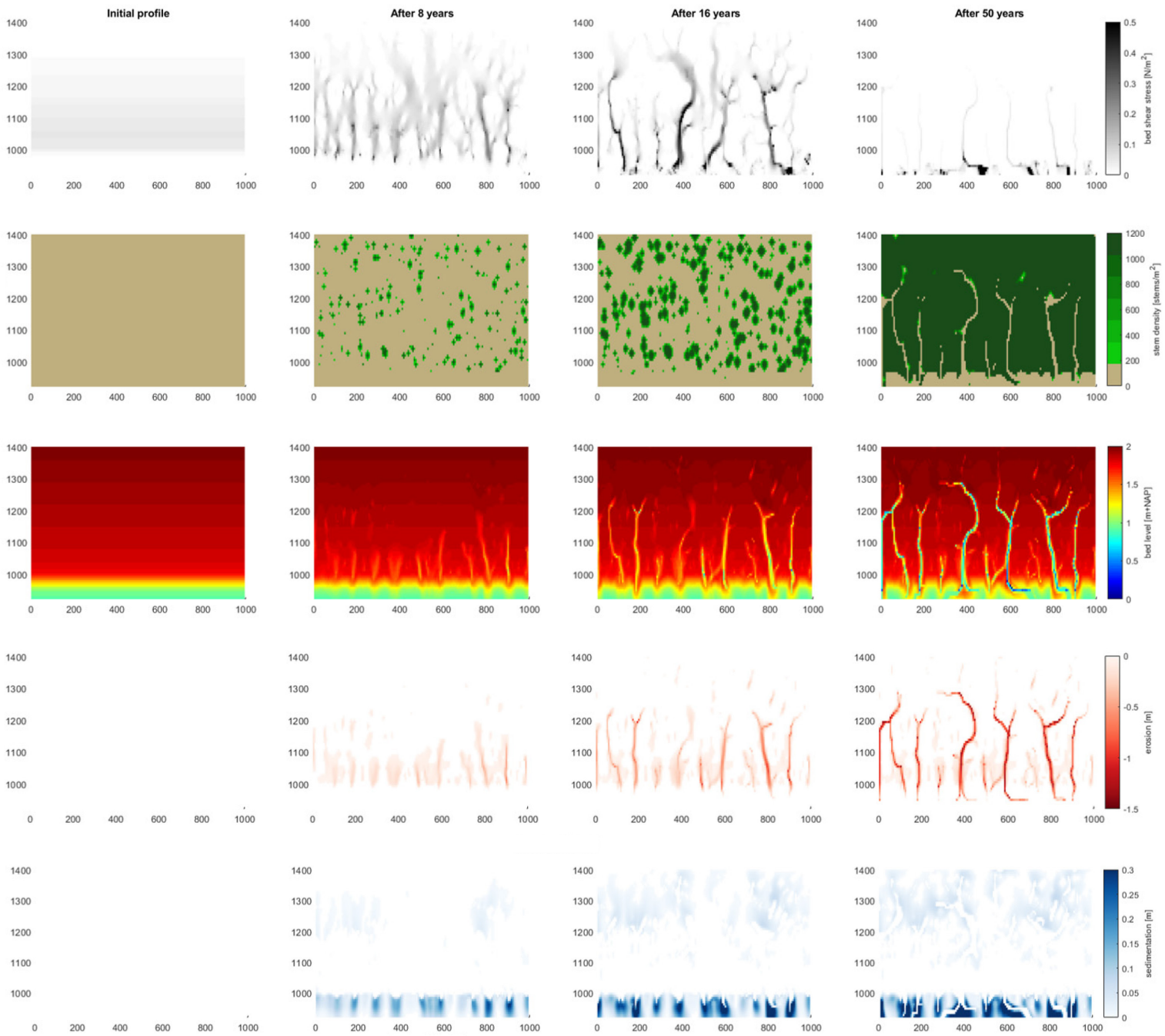


Figure 11 Bed shear stress, vegetation cover, bed level evolution, erosion and sedimentation over time for the default case. The presented bed shear stress is the 90% value of a fitted normal distribution over all bed shear stresses occurring during a single tidal cycle. Horizontal axes: domain width; vertical axes: domain length

## 3.2 Different vegetation rates

A sensitivity analysis was conducted on the seedling availability parameter (scenario 2). By altering this parameter the rate at which new vegetation pioneers onto the vegetation platform changes. In Figure 13 the vegetation and bed level development over time for different vegetation rates is shown. Larger plots of these results can be found in Appendix D. The default case showed that the morphological development is led by the development of the vegetation. This is also visible in Figure 13, as the different vegetation rates result in different morphological developments. All runs tend to develop towards an equilibrium state from an ecological viewpoint, similar to the default case, in which the vegetation is no longer able to further expand or pioneer. This is also visible by looking at the average stem density on the vegetated platform over time, see Figure 12. This average stem density plot can be interpreted as a total biomass plot in which the y-axis represents the total amount of biomass in the salt marsh. The total amount of biomass displays a logistic growth curve, similar to the growth curve of a single tussock (equation 7). The results with a vegetation rate of 4% and 8% show deep and narrow tidal channels which are nearly straight with respect to the direction of the tidal currents. In these runs the tidal channels have a width of single grid cell (7 metres). The 1% vegetation rate plot shows a more meandering tidal channel network with wider channels of around 2 grid cells (14 metres). As well, in the 1% vegetation bed level plot more side channels can be observed as opposed to the faster vegetation rates. Importantly, for all vegetation rates most of the tidal channels reach their maximum depth of 1.5 metre after 50 years of simulation. The time in which these depths are reached varies however. For the 8% vegetation rate this depth is reached after just 25 years. For the 1% vegetation rate it takes more than 37.5 years for the channels the reach these depths (see Figure 13).

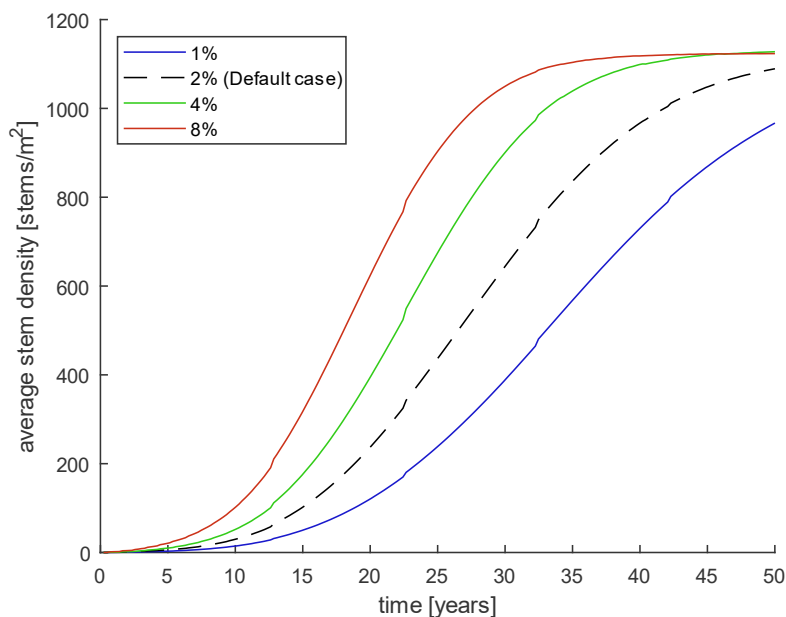


Figure 12 Average stem density over the vegetated platform for different vegetation rates (seedling availability)

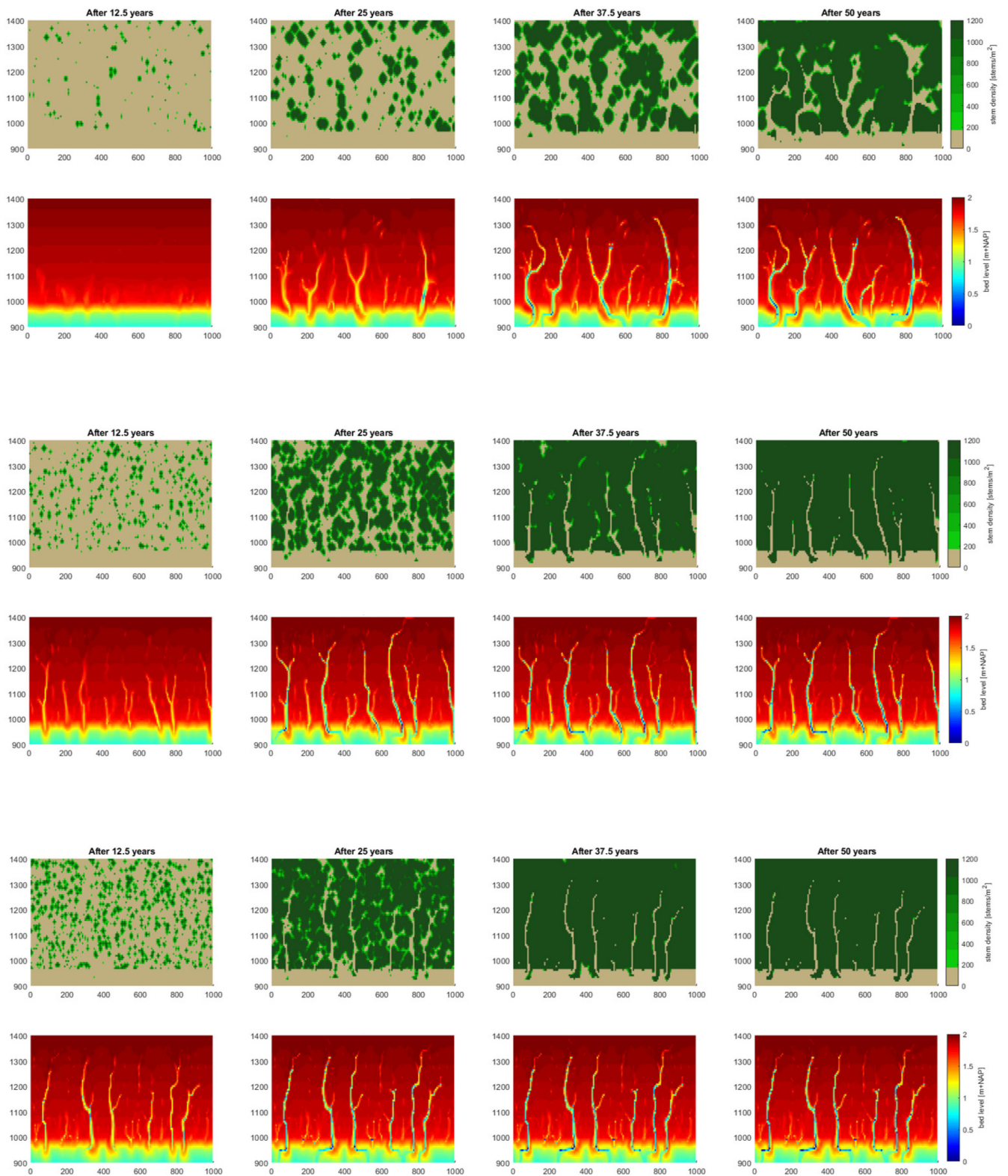


Figure 13 Vegetation field and bed level evolution for different vegetation rates. From top to bottom: 1%, 4% and 8% vegetation rate

### 3.3 Sea level rise

In order to study the response of the dynamic vegetation model to changes in the physical forcing over time a simple sea level rise scenario was run (scenario 3). The developed vegetation pattern and bathymetry of the default case after 50 years (see Figure 13) were used as the starting point for the sea level rise scenario. The model was forced with the same tidal boundary as in the default case (amplitude of 2.3 metres and period of 12 hour). A linear sea level rise of 1 metre over 100 years was added to this tidal boundary. Figure 15 displays the changes in vegetation cover over time. In Figure 14 and Figure 16, the erosion and sedimentation compared to the initial bathymetry are displayed. As the initial sediment thickness within the marsh was reset to 1.5 metres, this enabled further morphological development. Red colours indicate erosion, blue colours indicate sedimentation. A large deepening of the already existing tidal channels can be observed, see Figure 14. This suggest that the model is far from equilibrium from a morphological point of view.

As visible in Figure 15, after 50 years and a half metre of sea level rise a slight change in vegetation cover can be observed. The vegetation field has retracted slightly in the landward direction. Furthermore, vegetation coverage around the tidal channels is lost. As the sea level rises further the landward retraction in vegetation coverage further increases. Apart from the general landward retraction of the salt marsh further vegetation loss and erosion results in an expansion of the tidal channels that are already present. In other words, vegetation loss and subsequent further morphological development starts around the edge between tidal channel and vegetated platform. After 100 years, all vegetation has vanished. The loss of vegetation can be explained by looking at the formula governing inundation stress (see equation 9 and table 3). The critical inundation depth for *Spartina* vegetation is 1.1 metres. As the vegetated platform has an elevation of around 1.8 m+NAP this means that as soon as the water levels go over 2.9 m+NAP (1.8+1.1), vegetation will start to decay. The initial high water level is 2.3 m+NAP, with a SLR of 0.01 m per year such water levels would occur after around 60 years. The results indeed show that after around 60 to 70 years the decay of vegetation quickly increases (see Figure 15). Veel erosie

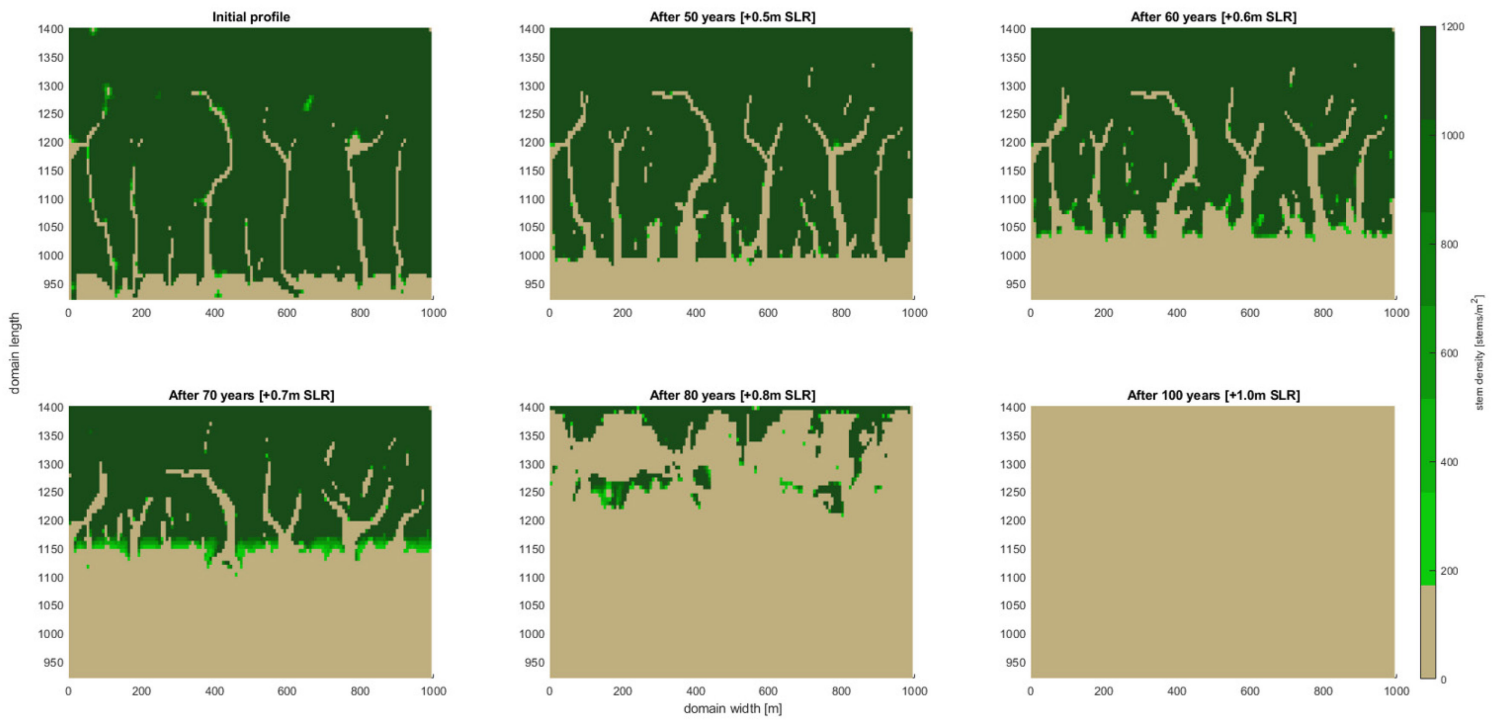


Figure 15 Vegetation pattern over time with a SLR rate of 0.01m per year

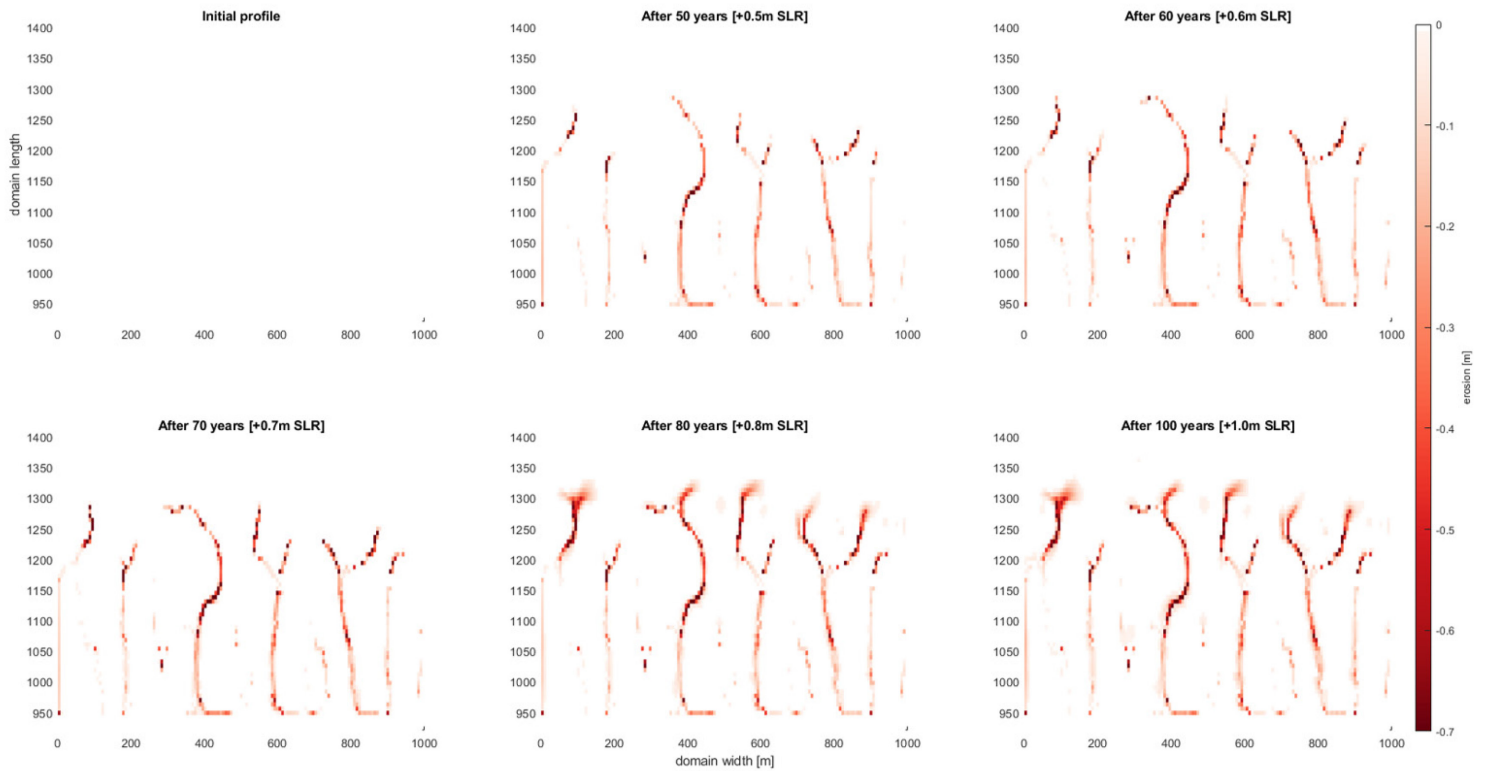


Figure 14 Erosion pattern over time with a SLR rate of 0.01m per year

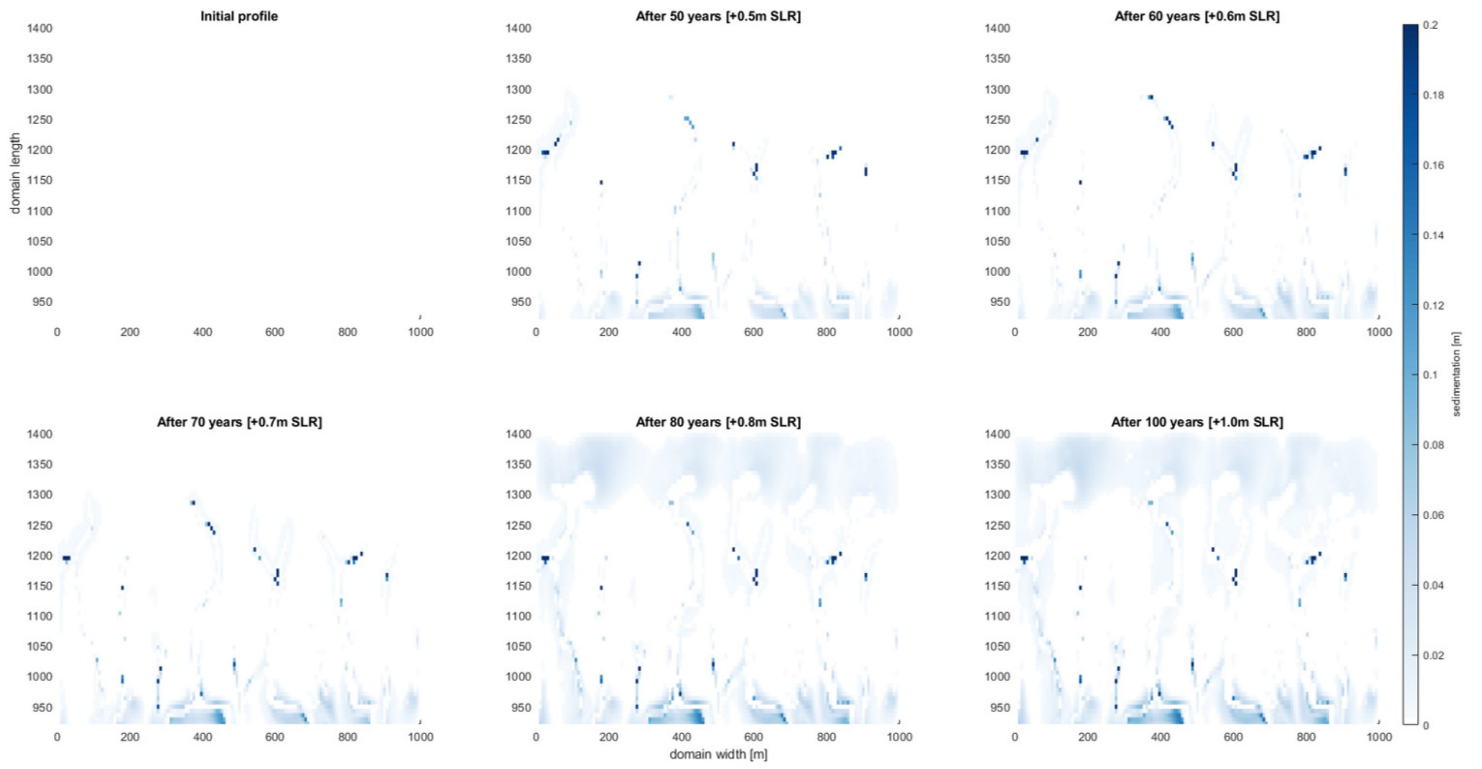


Figure 16 Sedimentation pattern over time with a SLR rate of 0.01m per year

## 4. Discussion

Similar to previous numerical salt marsh models (Best et al., 2018; Schwarz et al., 2018; Temmerman et al., 2007) the model results seem to suggest that the feedback mechanisms between vegetation and flowing water plays a vital role in the landscaping (i.e. the morphological and ecological characteristics) of salt marsh ecosystems. See for example Figure 11, the outlines of the location and shape of the tidal channels which are clearly visible in the vegetation cover and bathymetry plot after 50 years can already be roughly observed by looking at the bed shear stresses after just 8 years of development. The rate of vegetation establishment furthermore seems to influence the width, depth and shape of the tidal channels. However, it should be noted that these results were derived using an initial sediment thickness of 1.5 metre. As such, the maximum depth of the channels is limited to around 1.5 metres. As visible in Appendix C, for nearly all modelled vegetation rates this depth is reached. It seems that the model overestimates the amount of tidal channel erosion. Yet, the critical bed shear stress for erosion and the erosion parameter (See Table 1) seem valid as they are of similar magnitude as the previously mentioned numerical salt marsh models. It could be that the model overestimates the flow velocities within the tidal channels. By altering the roughness coefficient towards a rougher bed this could possibly be corrected. The high bed shear stresses on the mudflat after 50 years of development are most certainly incorrect and the result of high flow velocities during the falling tide. The flow velocities within the vegetated areas decrease to such extent that water is held within these areas even after the tides have fallen below the vegetated platform. Possibly the roughness predictor (Appendix C) is unable to accurately model the influence of vegetation on flow.

Importantly, several physical processes which are present in the Western Scheldt estuary are not included in the model. Waves, river discharge and inflow of suspended sediments are all neglected in the current model. As such, processes such as vertical marsh expansion in which the salt marsh traps the suspended sediments from the tidal waters are not visible in the model results. The model results show only a slight vertical salt marsh expansion at the landward side of the salt marsh as a result of sediment which is being brought into suspension from the eroding tidal channels. The morphological developments as such are merely a redistribution from the sediments present in the initial bathymetry as the only open boundary is located sufficiently far away from the morphological active area.

The goal of this thesis was to develop and implement a dynamic vegetation model in a hydro- and morphodynamic model, in this case D-Flow FM. The main novelty of this approach is that the establishment of new vegetation is facilitated (or hampered) by the amount of hydro- and morphodynamic activity. As such, the growth and decay of vegetation would differ for differing hydro- and morphodynamic conditions caused by (time varying) physical forcings. However, as the model is only forced by tides, and these tides are constant over time, the simulations develop towards a rather static equilibrium. The sea level rise scenario (see Figure 15) displays a dynamic reaction of the vegetation field to the time varying tidal boundary. As no inflow of suspended sediment and thus no vertical marsh expansion is present these results cannot be used to assess the resilience of salt marshes against rising sea levels. As in real world scenarios the balance between vertical marsh expansion and sea level rise determines whether a salt marsh may survive or not (Best et al., 2018). However, the scenario does show that the vegetation model works as expected as the vegetation slowly decays as a result of the increasing inundation

stresses (equation 9). As well, no pioneering vegetation establishes as the requirements of window 2 (2.5 days inundation free) are not met.

The biggest advantage of the approach taken, namely an online coupled dynamic vegetation model over conventional methods such as a static vegetation field or offline coupled models, would be that an online coupled model is potentially better in capturing the reaction of vegetation to time varying physical forcings. However, this remains a hypothesis as the current model does not contain time varying physical forcings. Therefore it is recommended to further investigate the applicability of online coupled models by including time varying physical forcings such as waves, winds, river discharges and inflow of suspended sediment. Likely, this would result in more morphodynamic activity during the development of the salt marsh from unvegetated tidal flat to full grown marsh. Subsequently this could lead to less vegetation establishment which could reduce the flow concentration between patches of vegetation (as there is less vegetation) resulting in less and/or shallower tidal channels.

The chosen method has some clear disadvantages as well. First of all, an online coupled hydrodynamic, morphodynamic and ecological model requires quite a bit of runtime. The total amount of runtime of course varies depending on the model domain size, grid sizes and included processes (waves, winds, tides etc.). Large model runtimes may make it difficult to perform multiple sensitivity analysis. As a consequence, nearly all of these models apply a morphological factor in which the morphological developments are multiplied in order to simulate long-term morphological development. As pointed out in the method (section 2.6) this causes some difficulty for the implementation of the ecological model as the morphological developments as well as the hydrodynamic conditions are both used as input parameters for the WoO model. To overcome this problem, a single tidal boundary was used whilst in reality, the Western Scheldt estuary is subjected to spring-neap tides. The use of a single tide as tidal boundary may potentially overestimate the morphological development as in a spring-neap case large parts of the salt marsh remain unsubmerged for multiple days, whilst with a single tide these locations are inundated every simulated day.

#### *Depth averaged model and vegetation parametrization*

The influence of vegetation on hydrodynamics is accounted for by means of a roughness predictor. With such method the flow resistance is parametrized by means of bed roughness. One of the underlying assumptions on which the representative roughness equations of Baptist et al. (2007) are based is that the modelled vegetation consist of randomly distributed rigid cylinders with uniform properties. In reality vegetation within salt marshes is not rigid but rather flexible and tends to bend with the flow, hereby decreasing the frontal area for drag. This method may thus overestimate the vegetation resistance and subsequently overestimate bed shear stresses and erosion rates.

Moreover, the current model is depth-averaged. In a depth averaged model there are no differences in the vertical velocity profile and the vertical velocity profile is assumed as uniform. Amongst other from flume experiments it is known that the vertical velocity profile in case of submerged vegetation is far from uniform, see for example Figure 17. Visualized is a uniform velocity profile within the vegetation and a logarithmic profile over the vegetation. The representative roughness equations (Appendix C) do contain different approximations for the case of submerged vegetation as opposed to unsubmerged vegetation. Following these equations, unsubmerged grid cells acquire a larger roughness as opposed to the submerged grid

cells with the same vegetation characteristics. Yet, a roughness predictor combined with a depth averaged model is unable to simulate a logarithmic profile over submerged vegetation. As such, the flow over vegetated grid cells is limited using the current model setup. This may explain why most of the sediment eroded from the channels is deposited in close proximity of these same channels, see Figure 11. In reality one might expect that flowing water can travel significant distances over submerged vegetation. Hereby bringing suspended sediment further in the marsh resulting in sedimentation further away from tidal channels. It therefore seems that the current model setup is less suitable for modelling flow routing and sedimentation patterns. For these processes, the difference in the vertical velocity profile is important and three dimensional numerical models would be better in recreating this process.

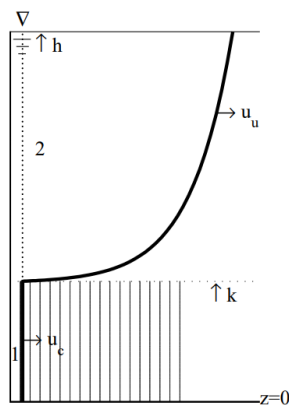


Figure 17 Schematised vertical velocity profile in case of submerged vegetation. Image adapted from Baptist et al. (2007)

To conclude, the model results show that it is possible to implement a process based vegetation model in a numerical salt marsh model. The results furthermore show that by doing so similar results are achieved as existing numerical salt marsh models. However, this seems to be the result of the limited forcing in the current setup in which only tides are included. By including more physical forcings, likely a more dynamic vegetation field will occur which can potentially aid in further studies on the decadal dynamic evolution of salt marshes.

Lastly, these model results show that the inclusion of a process based vegetation establishment model does not necessarily lead to different results as opposed to the existing stochastic establishment functions. This may be due to the fact that morphodynamic activity in general is low as the model is only forced by tides. However this could also be the result of the fact that in the current model approach the process based WoO model, which contains requirements on very small timescales (Window 1: 2.5 days inundation free, Window 2: 80 days of bed level dynamics within a threshold) is implemented into a model aiming the simulate very large timescales (decades). The modifications and adaptations made (see section 2.5 and 2.6) to enable this may be invalid.

## 4 Conclusions

The aim of this thesis was to study the physical processes driving the decadal dynamic behaviour of salt marshes. In line with this aim three research questions were established. In this section an answer will be given on each research question.

### 4.1 How can the influence of hydro- and morphodynamics on salt marsh vegetation dynamics, and specifically on the establishment of new vegetation, be included in a numerical model?

The developed model contains tides, sediment dynamics (sedimentation and erosion) and the influence of vegetation on flow. The model contains an online coupled dynamic vegetation model. The vegetation is updated for nearly every timestep, namely every hydrodynamic hour. The influence of hydro- and morphodynamics on salt marsh vegetation is modelled by means of two vegetation models which together form a dynamic vegetation model which accounts for the dynamic behaviour of salt marshes under the influence of hydro- and morphodynamics. The influence of hydrodynamics on established vegetation is modelled by means of the population dynamics concept of Temmerman et al. (2005). The establishment of new vegetation is modelled by the Windows of Opportunity concept developed by Poppema et al. (2019). This adapted version of the original Windows of Opportunity concept accounts for the notion that seedling failure may be a result of bed level changes as well as inundation stress. The population dynamics concept of Temmerman et al. (2005) contains logistic growth of vegetation, lateral diffusion of vegetation, decay of vegetation as a result of flow stress and lastly decay of vegetation as a result of inundation stress. The vegetation is modelled as a vegetation field consisting solely of *Spartina Anglica* vegetation and its typical physical properties.

### 4.2 How can we get confidence in the model results?

The model produces similar results as multiple existing numerical salt marsh models used for studying the decadal evolution of salt marshes. The colonization of salt marsh vegetation on bare intertidal areas suitable for vegetation growth such as mudflats is an important process for the long term morphological and ecological evolution of salt marshes. The gradual establishment of vegetation results in patches of vegetation. Within these patches flow velocities are reduced as a result of the drag forces caused by vegetation whilst in the unvegetated areas flow is concentrated between patches of vegetation which results in an increase of velocities and ultimately the formation of channels. This process is similar to what Temmerman et al. (2007) found.

The rate of vegetation establishment (e.g. the amount of seedlings available) influences the large scale vegetation pattern. Slow vegetation rates result in the creation of larger and shallower channels which show a meandering. Fast vegetation rates causes the creation of narrow and deep tidal channels which are nearly straight with respect to the tidal flow direction. These result seem similar to the results of Schwarz et al. (2018) in which it was found that rate of vegetation establishment combined with the amount of existing bed forms influences the morphological development and landscaping of salt marshes.

Lastly, the sea level rise scenario displayed that the dynamic vegetation model is capable of representing the reaction of salt marsh vegetation to increasing flow stresses as a result of higher and longer inundation periods. These results seems similar to those of Best et al. (2018) in which it was demonstrated that inundation heights higher than the critical inundation height for *Spartina* vegetation results in a landward retreat of the salt marsh.

#### 4.3 How can sea level rise be incorporated in a dynamic vegetation model, and how does this affect the salt marsh evolution?

Given the current model setup, and the characteristics of (2DH) numerical hydro- and morphodynamic models in general, a process based model is created. As such, sea level rise can quite easily be implemented in this model by increasing the mean water level of the tidal boundary condition over time. The sea level rise scenario showed that the vegetation model is capable of recreating the landward decrease of salt marsh vegetation as a result of the increase in hydrodynamic stress.

## 6. Recommendations

Based on the discussion and conclusions presented in the previous chapters the following recommendations can be identified.

It is recommended to further develop the current model by including time varying processes such as waves, inflow of suspended sediments and river discharges. The advantages of doing so would be twofold. Firstly, by including these processes likely a more dynamic vegetation field could be modelled. Eventually such model may be used to study which physical forcings (magnitude and/or combination of forcings) are responsible for the decadal salt marsh growth and retreat observed in practice (e.g. van der Wal et al., 2008; Huang et al., 2008). Secondly, by including inflow of suspended sediment the resilience of salt marshes against rising sea levels can be assessed.

In the current model setup the impact of vegetation on hydrodynamics is accounted for by means of a roughness predictor. This roughness predictor increases the bed roughness of vegetated grid cells. Other methods are available as well. For example the method of Uittenbogaard (2003). In this method the momentum equations are extended to account for the vegetation induced friction force generated by water flowing around these cylinders. Moreover, this method accounts for the obstruction of momentum exchange as a result of the area that is taken in by vegetation. In a model comparison study by Horstman et al. (2013) both methods were compared to study the differences in modelled hydro- and sediment dynamics in a mangrove creek catchment. The modelled sedimentation rates computed using the approach of Uittenbogaard (2003) agreed slightly better with field data as opposed to the sedimentation rates computed using the roughness predictor. It would be interesting to adapt the model presented in this thesis to a model in which vegetation is modelled following this approach. Most likely, this would alter the sedimentation and erosion patterns and thus possibly the vegetation establishment (since vegetation establishment is a function of amongst others bed level dynamics in the presented model). Disregarding the debate which of these methods is more accurate, it is recommended to study if a different method leads to different results. Either this further strengthens the conclusions drawn and validates the model approach. Or this could illustrate that vegetation parametrization is an important aspect in numerical salt marsh modelling. Possibly, this also reduces erosion rates as the high roughness in the vegetated areas seems to result in a large concentration of flow between unvegetated grid cells.

As mentioned in the results and the discussion the current model seems to overestimate tidal channel erosion. Currently this is managed by limiting the initial sediment thickness. The discussion mentions several processes which may be responsible for this overestimation. First of all the single tidal boundary results in daily hydrodynamic activity whilst in reality salt marshes in the Western Scheldt are subjected to spring-neap tides and thus inundated less frequently resulting in less hydro- and morphodynamic activity. Secondly, the roughness predictor used for the parametrization of vegetation resistance assumes that the vegetation field consists of rigid cylinders, whilst *Spartina Anglica* vegetation is known to bend with flowing water hereby decreasing the frontal area and overall vegetation induced drag. Lastly, the roughness coefficient can be altered towards a rougher bed which would reduce flow velocities and erosion rates in general. It is recommended to alter one or more of these aspects to study whether this reduces tidal channel erosion. Potentially this can lead to a more accurate result regarding the tidal channel depths.



## References

- Allen, J. R. L. (2000). Morphodynamics of Holocene salt marshes: A review sketch from the Atlantic and Southern North Sea coasts of Europe. *Quaternary Science Reviews*, 19(12), 1155–1231.
- Almeida, C. M. R., Mucha, A. P., & Teresa Vasconcelos, M. (2011). Role of different salt marsh plants on metal retention in an urban estuary (Lima estuary, NW Portugal). *Estuarine, Coastal and Shelf Science*, 91(2), 243–249.
- Attema, Y. (2014). Long-term Bio-geomorphological Modelling of the Formation and Succession of Salt Marshes. TU Delft, Delft University of Technology (2014)
- Baeyens, W., Van Eck, B., Lambert, C., Wollast, R., & Goeyens, L. (1997). General description of the Scheldt estuary. *Hydrobiologia*, 366, 1–14.
- Balke, T., Bouma, T. J., Horstman, E. M., Webb, E. L., Erftemeijer, P. L. A., & Herman, P. M. J. (2011). Windows of opportunity: Thresholds to mangrove seedling establishment on tidal flats. *Marine Ecology Progress Series*, 440, 1–9.
- Baptist, M. J., Babovic, V., Uthurburu, J. R., Keijzer, M., Mynett, A., Verwey, A., ... Keijzer, M. (2007). On inducing equations for vegetation resistance On inducing equations for vegetation resistance Sur l' établissement des équations traduisant la résistance due à la végétation. *Journal Of Hydraulic Research*, 45(5), 435–450.
- Best, Ü. S., Van der Wegen, M., Dijkstra, J., Willemsen, P. W. J. M., Borsje, B. W., & Roelvink, D. J. (2018). Do salt marshes survive sea level rise? Modelling wave action, morphodynamics and vegetation dynamics. *Environmental modelling & software*, 109, 152–166.
- Borsje, B. W., van Wesenbeeck, B. K., Dekker, F., Paalvast, P., Bouma, T. J., van Katwijk, M. M., & de Vries, M. B. (2011). How ecological engineering can serve in coastal protection. *Ecological Engineering*, 37(2), 113–122.
- Bouma, T. J., van Belzen, J., Balke, T., van Dalen, J., Klaassen, P., Hartog, A. M., ... Herman, P. M. J. (2016). Short-term mudflat dynamics drive long-term cyclic salt marsh dynamics. *Limnology and Oceanography*, 61(6), 2261–2275.
- Callaghan, D. P., Bouma, T. J., Klaassen, P., van der Wal, D., Stive, M. J. F., & Herman, P. M. J. (2010). Hydrodynamic forcing on salt-marsh development: Distinguishing the relative importance of waves and tidal flows. *Estuarine, Coastal and Shelf Science*, 89(1), 73–88.
- Cao, H., Zhu, Z., Balke, T., Zhang, L., & Bouma, T. J. (2018). Effects of sediment disturbance regimes on *Spartina* seedling establishment: Implications for salt marsh creation and restoration. *Limnology and Oceanography*, 63(2), 647–659.

- D'Alpaos, A., Lanzoni, S., Marani, M., & Rinaldo, A. (2007). Landscape evolution in tidal embayments: Modeling the interplay of erosion, sedimentation, and vegetation dynamics. *Journal of Geophysical Research: Earth Surface*, *112*(1), 1–17.
- Deltares (2019). D-Flow Flexible Mesh User Manual Version 1.5.0
- Drake, B. G. (1976). Seasonal Changes in Reflectance and Standing Crop Biomass in Three Salt Marsh Communities. *Plant Physiology*, *58*(5), 696 LP-699.
- Friess, D. A., Krauss, K. W., Horstman, E. M., Balke, T., Bouma, T. J., Galli, D., & Webb, E. L. (2012). Are all intertidal wetlands naturally created equal? Bottlenecks, thresholds and knowledge gaps to mangrove and saltmarsh ecosystems. *Biological Reviews*, *87*(2), 346–366.
- Harmsworth, G. C., & Long, S. P. (1986). An assessment of saltmarsh erosion in Essex, England, with reference to the Dengie Peninsula. *Biological Conservation*, *35*(4), 377–387.
- Horstman, E. M., Dohmen-Janssen, C. M., Bouma, T. J., & Hulscher, S. J. M. H. (2015). Tidal-scale flow routing and sedimentation in mangrove forests: Combining field data and numerical modelling. *Geomorphology*, *228*, 244–262.
- Horstman, E.M., Dohmen-Janssen, C.M. & Hulscher, S.J.M.H. (2013). Modeling tidal dynamics in a mangrove creek catchment in Delft3D. *Coastal Dynamics 2013 Proceedings*. 833-844.
- Hu, Z., Van Belzen, J., Van Der Wal, D., Balke, T., Wang, Z. B., Stive, M., & Bouma, T. J. (2015). Windows of opportunity for salt marsh vegetation establishment on bare tidal flats: The importance of temporal and spatial variability in hydrodynamic forcing. *Journal of Geophysical Research G: Biogeosciences*, *120*(7), 1450–1469.
- Huang, H. mei, Zhang, L. quan, Guan, Y. juan, & Wang, D. hui. (2008). A cellular automata model for population expansion of *Spartina alterniflora* at Jiuduansha Shoals, Shanghai, China. *Estuarine, Coastal and Shelf Science*, *77*(1), 47–55.
- Irmiler, U., Heller, K., Meyer, H., & Reinke, H.-D. (2002). Zonation of spiders and carabid beetles (Araneida, Coleoptera: Carabidae) in an inundation gradient of salt marshes at the North and Baltic Sea. *Biodiversity and Conservation*, *11*, 1129–1147.
- Kessel, T. Van, Vanlede, J., & Kok, J. De. (2011). Development of a mud transport model for the Scheldt estuary. *Continental Shelf Research*, *31*(10), S165–S181.
- Mariotti, G., & Fagherazzi, S. (2010). A numerical model for the coupled long-term evolution of salt marshes and tidal flats. *Journal of Geophysical Research: Earth Surface*, *115*(1), 1–15.
- Mcowen, C., Weatherdon, L., Bochove, J.-W., Sullivan, E., Blyth, S., Zockler, C., ... Fletcher, S. (2017). A global map of saltmarshes. *Biodiversity Data Journal*, *5*, e11764.

- Möller, I., Kudella, M., Rupprecht, F., Spencer, T., Paul, M., Van Wesenbeeck, B. K., ... Schimmels, S. (2014). Wave attenuation over coastal salt marshes under storm surge conditions. *Nature Geoscience*, 7(10), 727–731.
- Partheniades, E. (1965). Erosion and deposition of cohesive soils. *Journal of Hydraulics Division*, 91(1), 105-139.
- Poppema, D. W., Willemsen, P. W. J. M., de Vries, M. B., Zhu, Z., Borsje, B. W., & Hulscher, S. J. M. H. (2019). Experiment-supported modelling of salt marsh establishment. *Ocean & Coastal Management*, 168, 238–250.
- Roman, C. T., & Burdick, D. M. (n.d.). *Tidal marsh restoration: a synthesis of science and management*. Washington: Island Press.
- Sánchez, J. M., SanLeon, D. G., & Izco, J. (2001). Primary colonisation of mudflat estuaries by *Spartina maritima* (Curtis) fernald in Northwest Spain: Vegetation structure and sediment accretion. *Aquatic Botany*, 69(1), 15–25.
- Schwarz, C., van de Koppel, J., Zhu, Z., Ruessink, G., Temmerman, S., van Belzen, J., ... Bouma, T. J. (2018). Self-organization of a biogeomorphic landscape controlled by plant life-history traits. *Nature Geoscience*, 11(9), 672–677.
- Struyf, E., Dausse, A., Van Damme, S., Bal, K., Gribsholt, B., Boschker, H. T. S., ... Meire, P. (2006). Tidal marshes and biogenic silica recycling at the land-sea interface. *Limnology and Oceanography*, 51(2), 838–846.
- Temmerman, S., Bouma, T. J., Van de Koppel, J., Van der Wal, D., De Vries, M. B., & Herman, P. M. J. (2007). Vegetation causes channel erosion in a tidal landscape. *Geology*, 35(7), 631–634.
- Temmerman, S., Bouma, T. J., Govers, G., Wang, Z. B., De Vries, M. B., & Herman, P. M. J. (2005). Impact of vegetation on flow routing and sedimentation patterns: Three-dimensional modeling for a tidal marsh. *Journal of Geophysical Research: Earth Surface*, 110(4), 1–18.
- Temmerman, S., Govers, G., Meire, P., & Wartel, S. (2003). Modelling long-term tidal marsh growth under changing tidal conditions and suspended sediment concentrations, Scheldt estuary, Belgium. *Marine Geology*, 193(1–2), 151–169.
- Uittenbogaard, R.E., 2003. Modelling turbulence in vegetated aquatic flows. *Unpublished Results. Riparian Forest Vegetated Channels*. 1-17. Trento, Italy
- Van Eerden, M. R., Drent, R. H., Stahl, J., & Bakker, J. P. (2005). Connecting seas: Western Palaearctic continental flyway for water birds in the perspective of changing land use and climate. *Global Change Biology*, 11(6), 894–908.

- Vuik, V., Suh Heo, H. Y., Zhu, Z., Borsje, B. W., & Jonkman, S. N. (2018). Stem breakage of salt marsh vegetation under wave forcing: A field and model study. *Estuarine, Coastal and Shelf Science*, 200, 41–58.
- Wesenbeeck, B. K. van (2007). *Thresholds and shifts: Consequences of habitat modification in salt-marsh pioneer zones*. University of Groningen and Netherlands Institute for Ecology (NIOO-KNAW).
- Willemsen, P. W. J. M., Borsje, B. W., Hulscher, S. J. M. ., Van der Wal, D., Zhu, Z., Oteman, B., ... Bouma, T. J. (2018). Quantifying bed level dynamics at the transition of tidal flat and salt marsh : can we understand the lateral location of the marsh edge? *Journal of Geophysical Research: Earth Surface*.
- Williams, P., & Faber, P. (2001). Salt Marsh Restoration Experience in San Francisco Bay. *Journal of Coastal Research*, (27), 203–211.
- Van der Wal, D., Wielemaker-Van den Dool, A., & Herman, P. M. J. (2008). Spatial patterns, rates and mechanisms of saltmarsh cycles (Westerschelde, The Netherlands). *Estuarine, Coastal and Shelf Science*, 76(2), 357–368.

## Appendix A – Hydrodynamic model equations

The momentum equations in x- and y- direction included in the D-Flow FM model are given by equations A.1 and A.2. The depth-averaged continuity equation is given in equation A.3

$$\frac{\partial u}{\partial t} + u \frac{\partial u}{\partial x} + v \frac{\partial u}{\partial y} - fu = -\frac{1}{\rho_0} P_u - \frac{gu\sqrt{u^2 + v^2}}{C^2 h} + F_x + F_{sx} + M_x \quad (\text{A. 1})$$

$$\frac{\partial v}{\partial t} + u \frac{\partial v}{\partial x} + v \frac{\partial v}{\partial y} + fv = -\frac{1}{\rho_0} P_v - \frac{gv\sqrt{u^2 + v^2}}{C^2 h} + F_y + F_{sy} + M_y \quad (\text{A. 2})$$

$$\frac{\partial h}{\partial t} + \frac{\partial hu}{\partial x} + \frac{\partial hv}{\partial y} = Q \quad (\text{A. 3})$$

In which,

Parameter	Description	Value [unit]
u, v	Depth averaged velocity components in x and y direction respectively along the Cartesian axis	[m s <sup>-1</sup> ]
h	Water depth	[m]
g	Gravitational acceleration	9.81 [ms <sup>-2</sup> ]
$\rho_0$	Water density	1000 [kg m <sup>-3</sup> ]
f	Coriolis coefficient	2 $\Omega$ sin( $\theta$ ) [rad s <sup>-1</sup> ]
P	Pressure gradient	[N m <sup>-2</sup> ]
C	Chézy coefficient	[m <sup>1/2</sup> s <sup>-1</sup> ]
$F_x, F_y$	Horizontal diffusive forces	[N kg <sup>-1</sup> ]
$F_{sx}, F_{sy}$	Secondary flow forces	[N kg <sup>-1</sup> ]
$M_x, M_y$	Sources and sinks of momentum (e.g. discharge, dams, groynes or wave stresses)	[N kg <sup>-1</sup> ]
Q	Discharge	[m <sup>3</sup> s <sup>-1</sup> ]

As the size of the model domain is small compared to the scale at which Coriolis force has a significant effect on flow the effect of the earth's rotation on flow is ignored. The water density is assumed as constant over time and thus density driven flow is not included. The model does not include dams, groynes, waves or other sources and sinks of momentum. Hence the momentum equations effectively reduce to:

$$\frac{\partial u}{\partial t} + u \frac{\partial u}{\partial x} + v \frac{\partial u}{\partial y} = -\frac{gu\sqrt{u^2 + v^2}}{C^2 h} + F_x + F_{sx} \quad (\text{A. 4})$$

$$\frac{\partial v}{\partial t} + u \frac{\partial v}{\partial x} + v \frac{\partial v}{\partial y} = -\frac{gv\sqrt{u^2 + v^2}}{C^2 h} + F_y + F_{sy} \quad (\text{A. 5})$$

And as such, the model includes energy dissipation due to bottom roughness, diffusion of flow and secondary flow. For the exact equations governing the diffusion of flow and secondary flow ( $F_x, F_y, F_{sx}, F_{sy}$ ) kindly see the D-Flow FM manual (Deltares, 2019).

## Appendix B – Discretization of vegetation diffusion equation

The lateral diffusion of vegetation as described in equation 6 is discretised by equation B.1. This equation is based on the work of Attema (2014), yet altered to be suitable for structured grids instead of the original equation which was designed for triangular grids.

$$\left(\frac{\partial n_b}{\partial t}\right)_{diff} = \frac{\sum_{i=1}^{i=4} D * \max\{n_{b,i} - n_b, 0\} * L}{A} * \Delta t \quad (\text{B.1})$$

In which,

Parameter	Description	Value [unit]
$n_b$	Stem density in grid cell	[stems m <sup>-2</sup> ]
$n_{b,i}$	Stem density in neighbouring grid cells	[stems m <sup>-2</sup> ]
D	Diffusion coefficient	0.2 [m yr <sup>-1</sup> ]
L	Length of the interface between grid cells	7 [m]
A	Grid cell area	7*7 [m <sup>2</sup> ]
$\Delta t$	Time step w.r.t. diffusion coefficient	[-]

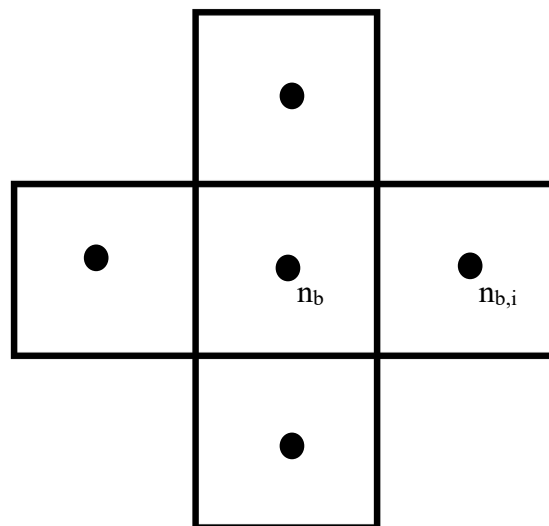


Figure 18 The change in stem density in a given grid cell as a result of diffusion is determined by the difference between its own stem density and the stem densities in the four neighbouring grid cells

## Appendix C – Vegetation in the hydrodynamic model

The influence of vegetation in the hydro- and morphodynamic model is accounted for by the means of the roughness predictor similar to the roughness predictor as proposed by Baptist et al. (2007). The roughness predictor accounts for the presence of vegetation by increasing the bed roughness in vegetated areas. Two predictors are used, one in the case of unsubmerged vegetation and one for submerged vegetation. The equation for submerged vegetation is presented in equation C.1, the equation for unsubmerged vegetation is presented in equation C.2.

$$C = \frac{1}{\sqrt{\frac{1}{C_b^2} + \frac{C_D n D h_v}{2g}}} + \frac{\sqrt{g}}{\kappa} \ln\left(\frac{h}{h_v}\right) \quad (\text{C. 1})$$

$$C = \frac{1}{\sqrt{\frac{1}{C_b^2} + \frac{C_D n D h_v}{2g}}} \quad (\text{C. 2})$$

In which,

Parameter	Description	Value [unit]
C	Representative Chézy roughness	[m <sup>1/2</sup> s <sup>-1</sup> ]
C <sub>b</sub>	Alluvial bed roughness	[m <sup>1/2</sup> s <sup>-1</sup> ]
C <sub>D</sub>	Vegetation drag coefficient	0.7 [-]
n	Vegetation density	[stems m <sup>-2</sup> ]
h <sub>v</sub>	Height of a vegetation stem	0.5 [m]
D	Diameter of vegetation stem	0.003 [m]
g	Gravitational acceleration	9.81 [m s <sup>-2</sup> ]
κ	Von Kármán constant	0.4 [-]
h	Water level	[m]
u	Flow velocity	[m s <sup>-1</sup> ]
n <sub>m</sub>	Manning coefficient	0.023 [s m <sup>-1/3</sup> ]

The alluvial bed roughness is determined using the manning coefficient which translates to a bed roughness using equation C.3

$$C_b = \frac{\sqrt[6]{h}}{n_m} \quad (\text{C. 3})$$

## Appendix D – Bed level and vegetation evolution over time for different vegetation rates

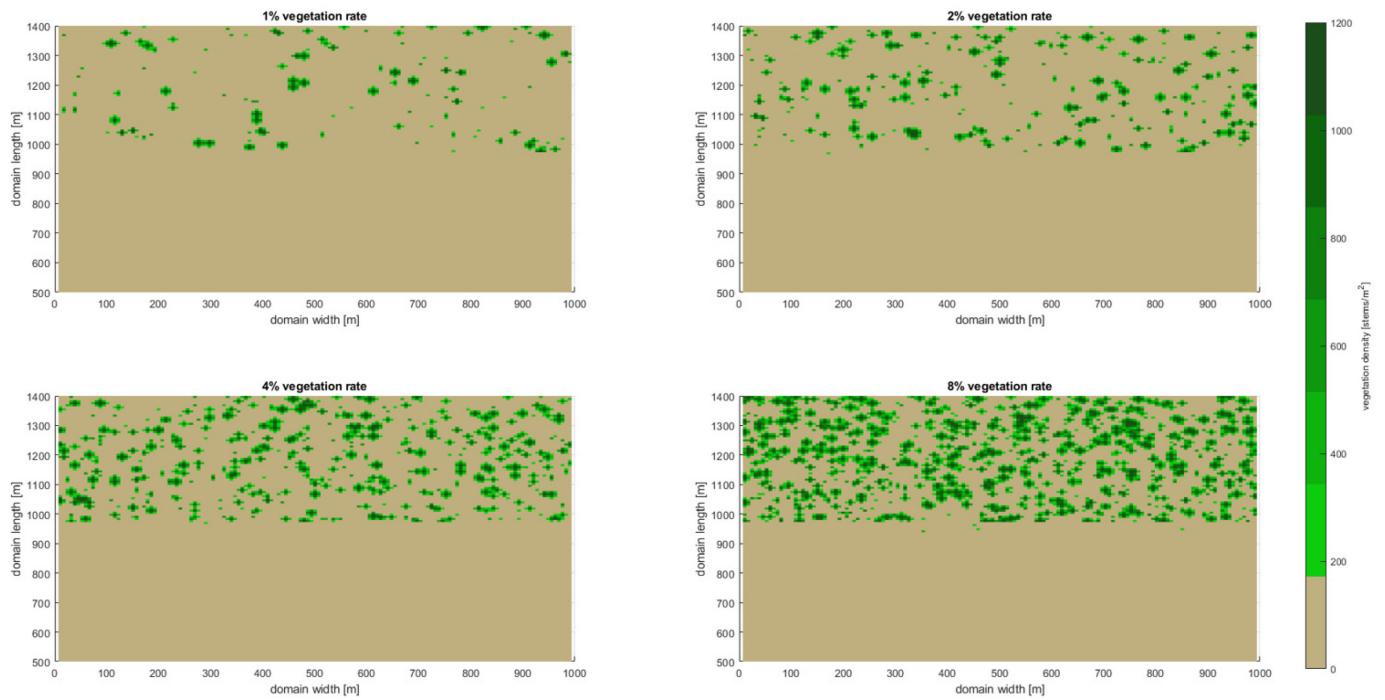


Figure 19 Modelled stem densities after 12 years

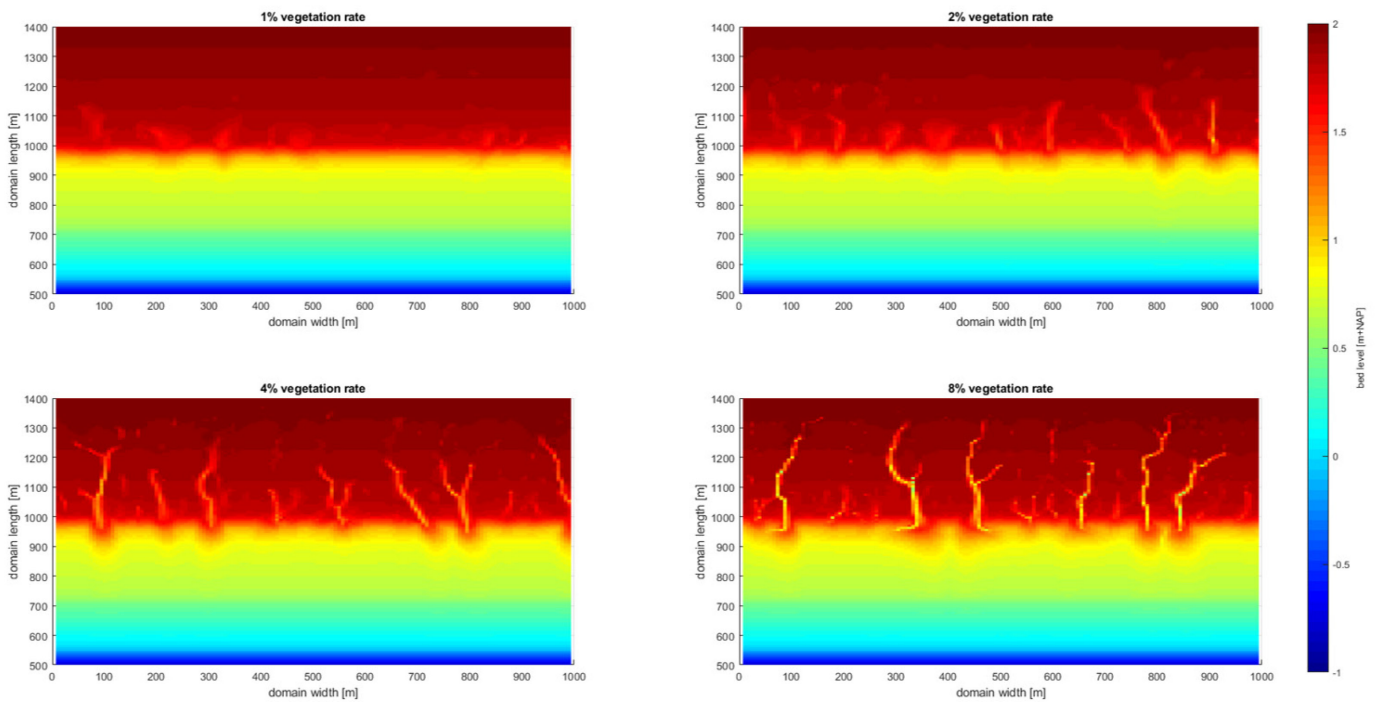


Figure 20 Modelled bed levels after 12 years

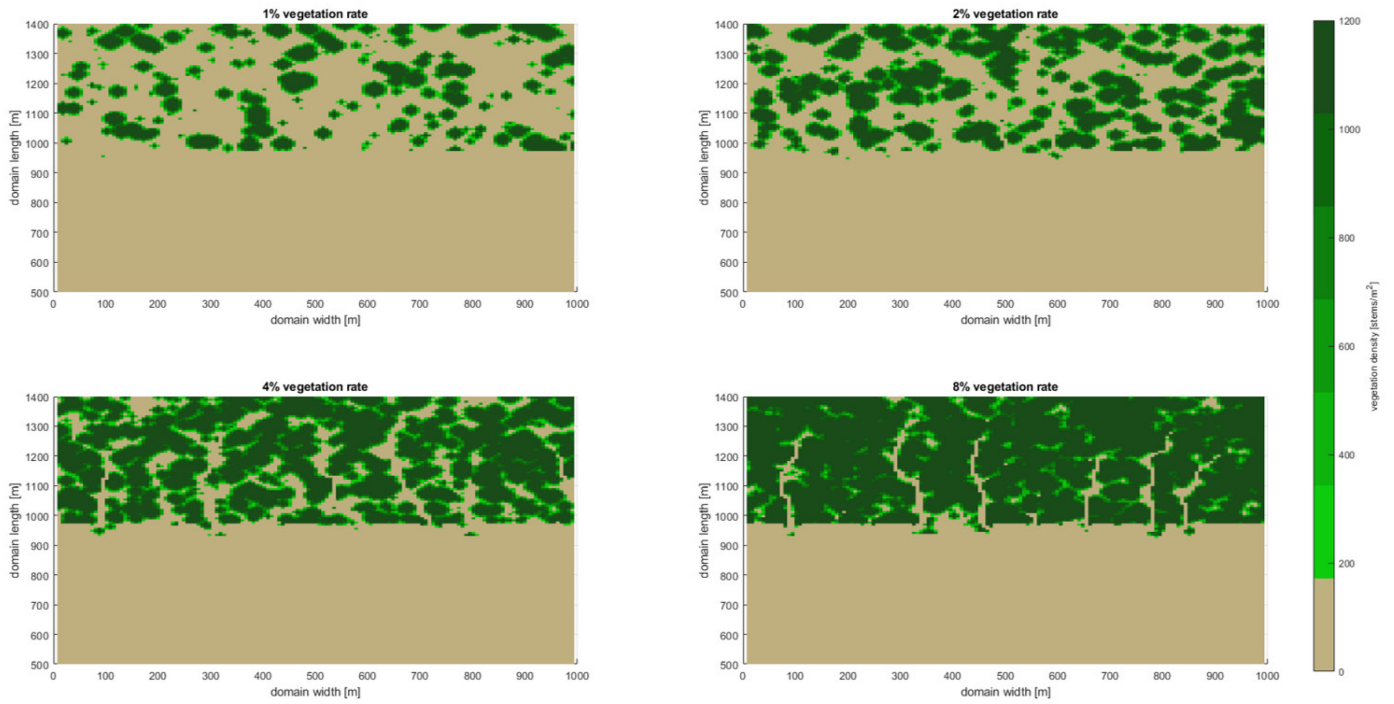


Figure 21 Modelled stem densities after 25 years

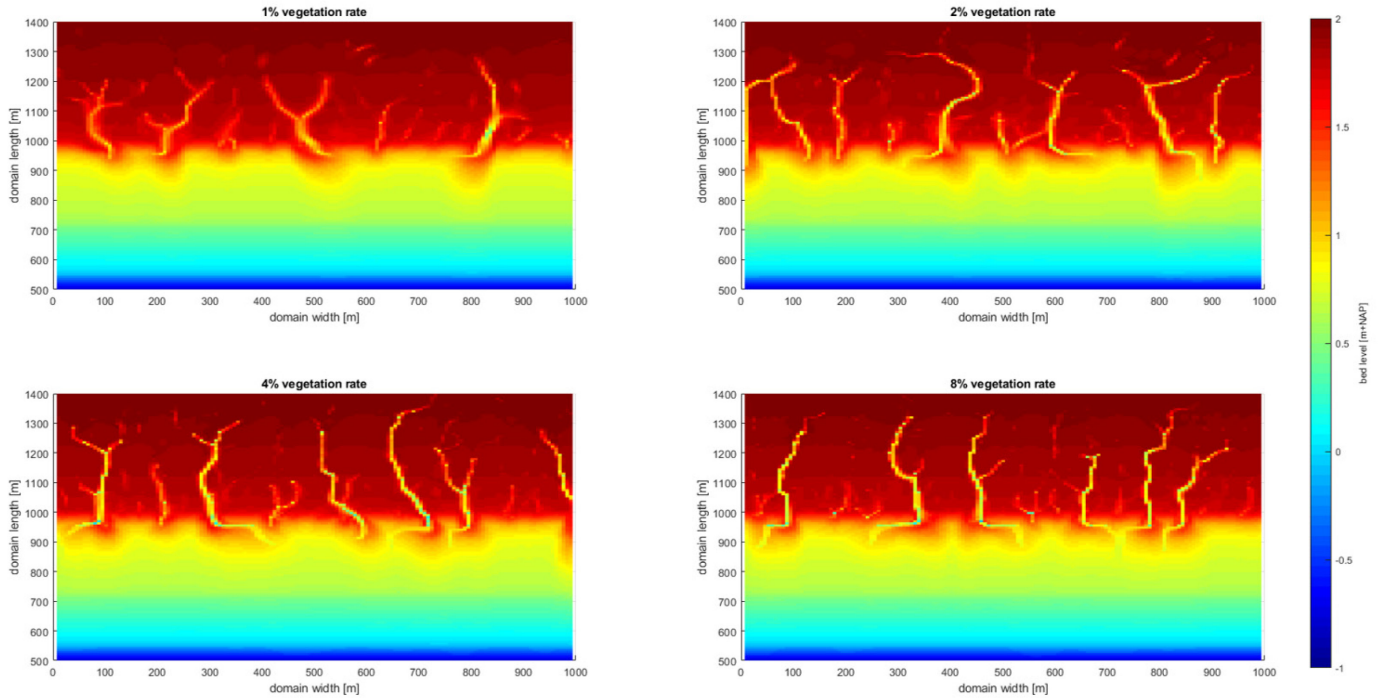


Figure 22 Modelled bed levels after 25 years

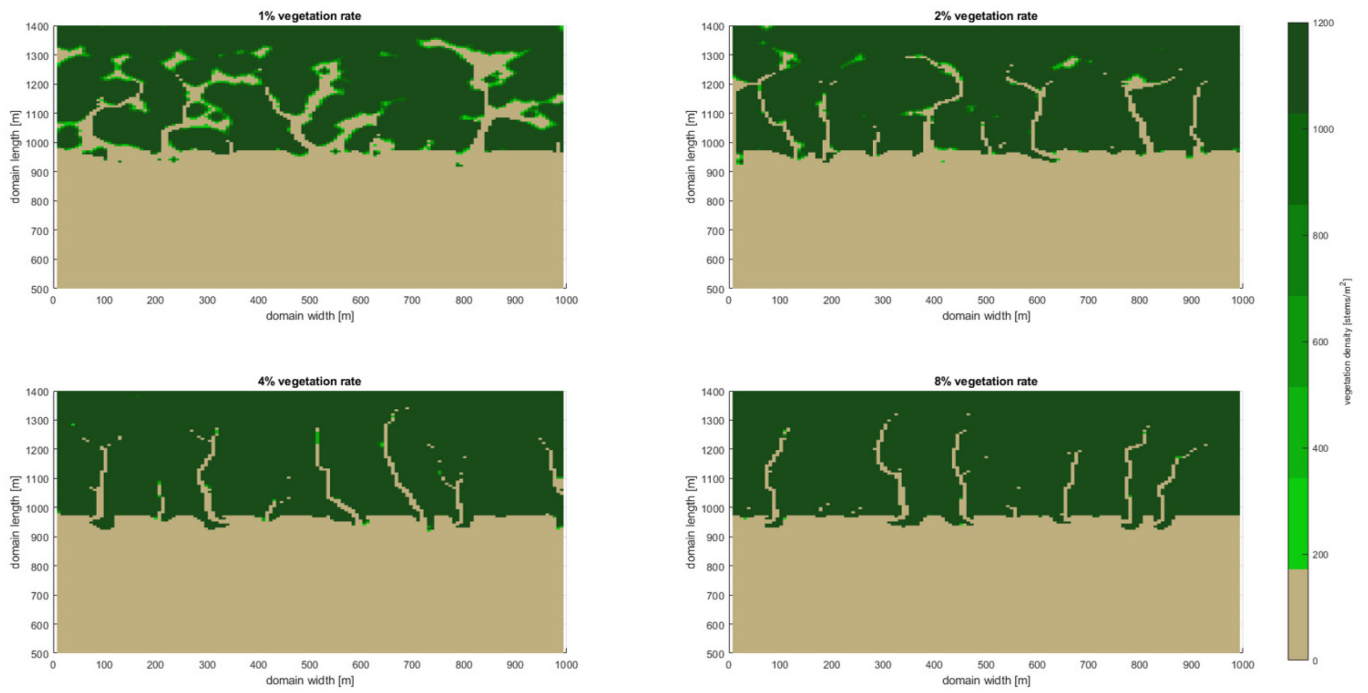


Figure 23 Modelled stem densities after 50 years

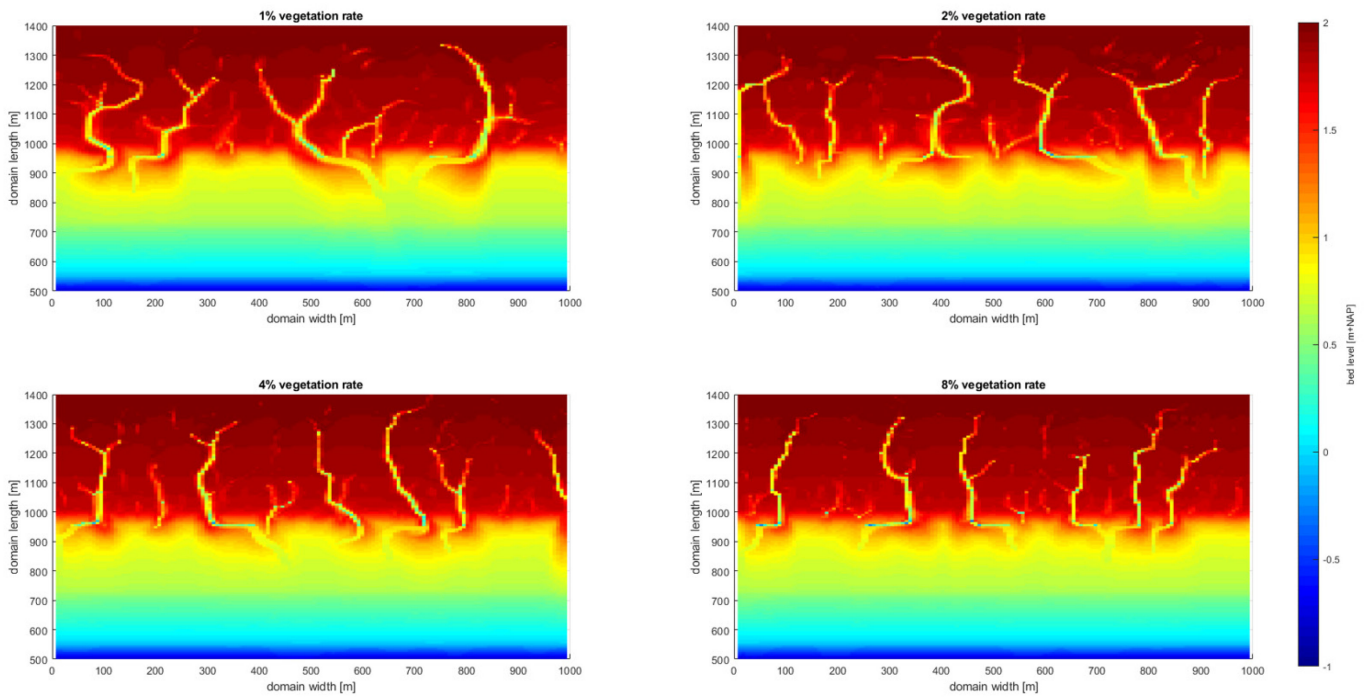


Figure 24 Modelled bed levels after 50 years